

# Rationalizing Product Formation in Piperazine Degradation: A Computational Study

Christopher Parks,\* Kevin Hughes, and Mohamed Pourkashanian



Cite This: *Ind. Eng. Chem. Res.* 2021, 60, 12864–12882



Read Online

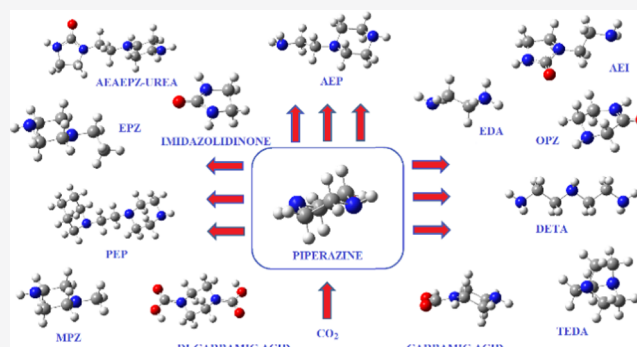
ACCESS |

Metrics & More

Article Recommendations

Supporting Information

**ABSTRACT:** Knowledge of the origins of degradation products observed during amine degradation is crucial to developing new, more efficient amines for future carbon-capture plants. Here, we report on a series of density functional theory (DFT) calculations rationalizing the routes to products observed from piperazine degradation studies. Experimentally viable routes to the formation of 1-(2-aminoethyl)-2-imidazolidinone (AEI), *N*-(2-aminoethyl)piperazine (AEP), 1-[2-[(2-aminoethyl)amino] ethyl] piperazine (AEAEpz), *N*-(2-hydroxyethyl)piperazine (HEP), and 1,1'-(1,2-ethanediyl)bis-piperazine (PEP) are presented. The modeling studies reported here are essential for the construction of chemical kinetic mechanisms, which can predict the byproduct formation from thermal and oxidative degradation.



## 1. INTRODUCTION

Global temperatures have risen significantly over the last 100 years. In part, this is attributed to an increase in the concentration of greenhouse gases in the atmosphere.<sup>1</sup> Hence, mitigating the adverse effects of carbon dioxide buildup is critically important. To date, one of the most promising and well-studied technologies is amine-based post-combustion carbon capture and storage.<sup>2,3</sup> Here, flue gas is passed through an amine solution, allowing the CO<sub>2</sub> to be absorbed. The gas can then subsequently be removed and stored or put to other uses.

The effectiveness of carbon-capture technology can be finely tuned by the choice of the solvent system. Ideally, the perfect amine would have resistance to oxidative and thermal degradation, have high CO<sub>2</sub> absorption capacity, rapid and reversible absorption kinetics, be economically viable, and have low volatility. The industrially applied standard for this application is currently monoethanolamine (MEA), which satisfies many of the aforementioned requirements to be a good solvent. However, many other amines have been studied for use in carbon capture including but not limited to 2-amino-2-methyl-1-propanol (AMP),<sup>4</sup> ethanolamine (DEA),<sup>5,6</sup> ethylenediamine (EDA),<sup>7–9</sup> methyldiethanolamine (MDEA),<sup>10</sup> morpholine (Mor),<sup>11–13</sup> and piperazine (Pip).

Piperazine is a cyclic secondary diamine that has been investigated for its applicability toward this technology. It is reported to have many advantages compared to MEA. It has a lower volatility, so less amine escapes into the atmosphere. It is thermally stable, up to temperatures of 150 °C.<sup>17</sup> Higher stripper pressures can also be tolerated compared to MEA. One of the greatest advantages is the higher CO<sub>2</sub> absorption capacity due to two amine groups on each piperazine molecule. Such

advantages led to a piperazine/AMP blend being suggested as a new industry standard.<sup>18</sup>

However, despite these advantages, the use of piperazine does have drawbacks. It is less soluble than MEA and can form a hexahydrate solid at room temperatures. Heating above 40 °C or binding to CO<sub>2</sub> aids dissolution. This observation means piperazine is generally used in a mixture with other amines. Moreover, piperazine is more expensive than MEA, which inhibits its widespread applicability.

The thermal and oxidative degradation of amine solvents represents a significant issue. Indeed, the cost of solvent degradation is often quoted to be as high as 10% of the total cost of CO<sub>2</sub> capture.<sup>19</sup> Moreover, the formation of unknown degradation products, which can potentially be vented into the atmosphere postcapture can have unknown health implications for both fauna and flora. The amine lost through degradation needs replacement periodically, which increases cost. Consequently, a thorough understanding of what products form and how they form is crucial to developing a suitable amine, which is resistant to such degradation.

To investigate the products formed during thermal degradation, Freeman and co-workers carried out degradation studies of CO<sub>2</sub>-loaded piperazine across the temperature range

Received: July 20, 2021

Revised: August 16, 2021

Accepted: August 17, 2021

Published: August 27, 2021



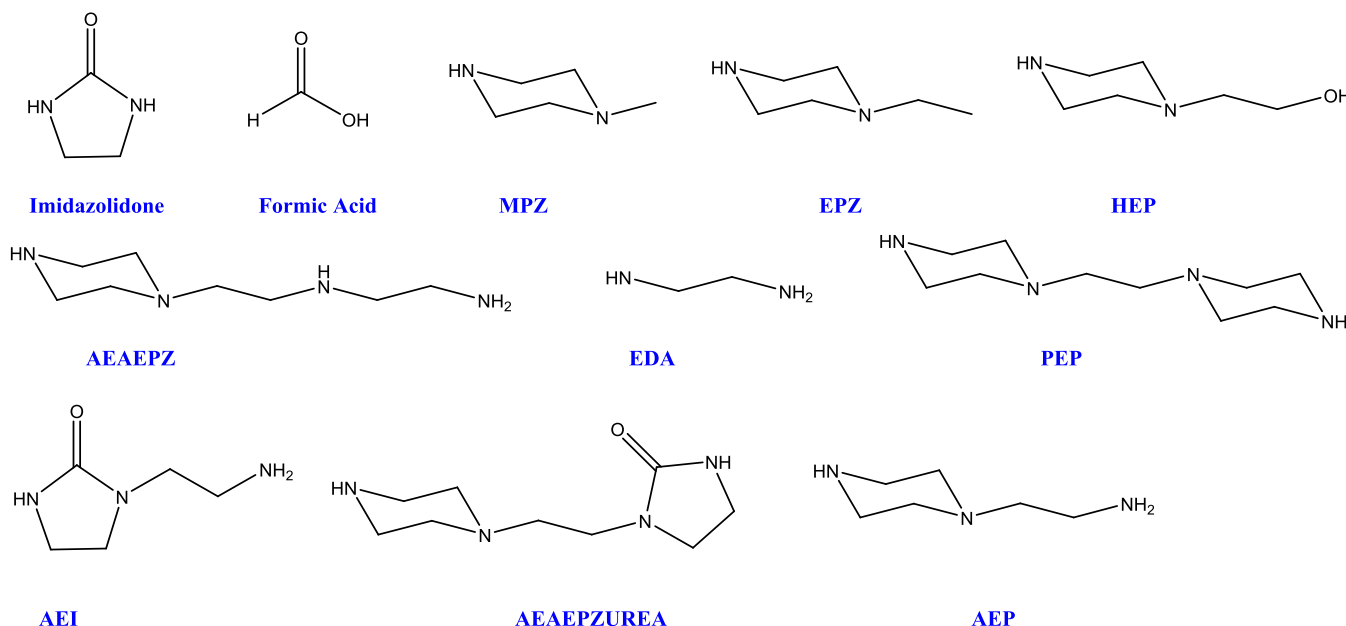
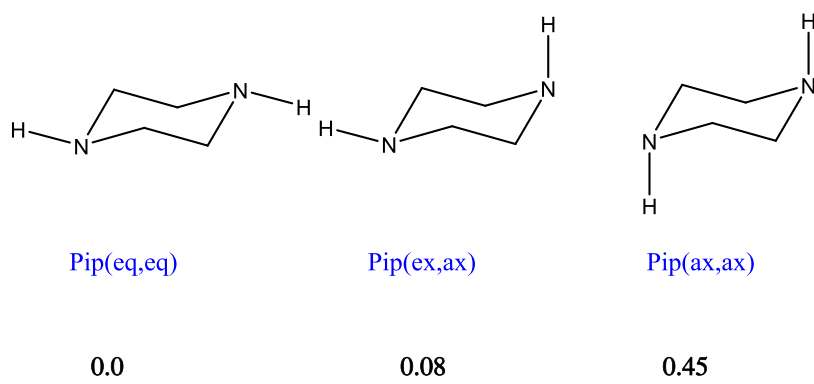


**Figure 1.** Major degradation products originating from thermal degradation of piperazine.

**Scheme 1.** Three Conformers of Piperazine and their Relative Energies (kcal mol<sup>-1</sup>)



of 135–170 °C.<sup>20</sup> The major products identified are summarized in Figure 1. Imidazoles, amides, carboxylates, ureas, and polymeric amine species were all characterized.

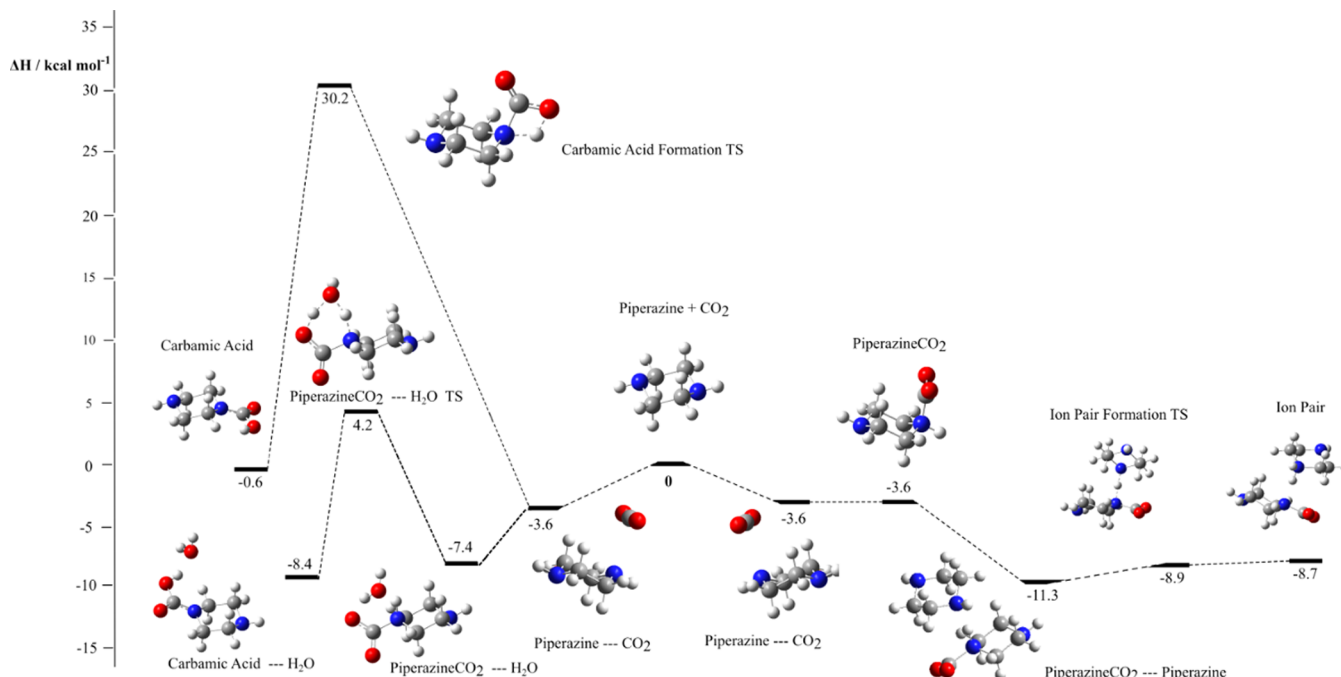
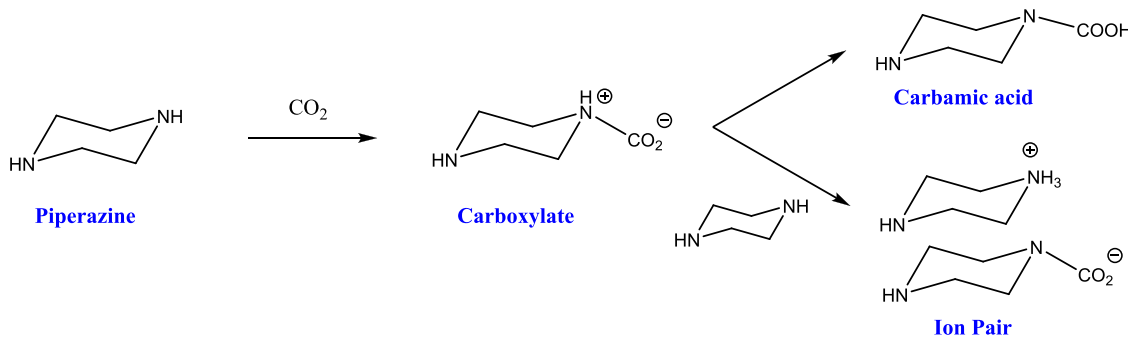
The number of indepth computational studies that have investigated amine degradation remains low in comparison to experimental studies. A number of studies have focussed purely on the carbon-capture step rather than considering degradation species.<sup>21–24</sup> Vavelstad et al.<sup>25</sup> calculated the free energies of formation of some of the most common degradation products, while Saeed et al. reported on the formation of imidazolidine species.<sup>26</sup> More recently, Yoon et al. reported ab initio molecular dynamics (AIMD) simulations looking into the elementary reactions of thermal degradation of amines.<sup>27</sup> They concluded that the formation of OZD, HEEDA, and N-(2-aminoethyl)-N'-(2-hydroxyethyl)imidazolidin-2-one (HEIA) is thermodynamically favorable. We recently reported on mechanistic routes to the common degradation products of MEA.<sup>28</sup>

In this paper, we use DFT to investigate the formation of many organic species resulting from the thermal and oxidative degradation of piperazine. Mechanisms are postulated and subsequently modeled to rationalize the formation of many of the reported degradation products of piperazine.

## 2. COMPUTATIONAL DETAILS

DFT calculations were performed by Gaussian 09 software, version D.01,<sup>29</sup> using Gaussian-supplied versions of BLAS and ATLAS. All calculations used the B3LYP functional.<sup>23,30</sup> The cc-pVTZ basis set was used for all elements.<sup>31</sup> This setup was chosen to be consistent with previously published work within the group and to allow for comparisons with that work.<sup>28</sup> Moreover, benchmarking studies have shown this setup to be similar in quality to that afforded by CCSD(T) calculations.<sup>32,33</sup> Further investigations using the m06 functional and def2TZVP basis set are presented in Table S1 in the Supporting Information.<sup>34</sup> In all calculations, the solvent was accounted for by the polarizable continuum model (PCM) method using solvent parameters for water as implemented in Gaussian.<sup>35</sup> Calculations were carried out at 298.15 K. Empirical dispersion corrections through the GD3 keyword were applied to all calculations.<sup>36</sup> Geometry optimizations were confirmed to be local minima by the absence of imaginary frequencies in the vibrational spectra. Transition states were optimized using the QST3 method as implemented in Gaussian.<sup>37</sup> All transition states were confirmed both visually via the presence of one large imaginary frequency corresponding to the saddle point and via intrinsic reaction coordinate (IRC) scans. An ultrafine grid was employed for all calculations with no symmetry constraints.

Scheme 2. Suggested Formation of both Carbamic Acid and an Ion Pair Species from Piperazine

Figure 2. DFT-calculated  $\Delta H$  energy profile for the proposed formation of an ion pair and carbamic acid from the reaction of  $\text{CO}_2$  and piperazine.

Radical species were calculated as singlets with the highest occupied molecular orbital (HOMO) and lowest unoccupied molecular orbitals (LUMOs) mixed (guess = mix option) to break the symmetry of the system unless stated otherwise. Free energies were calculated using the Grimme quasiharmonic entropy correction using the GoodVibes script.<sup>38</sup> All free activation energies are provided in Table S1 in the Supporting Information. Activation energies are calculated as the energy difference between the transition state and both reactants at infinite separation.

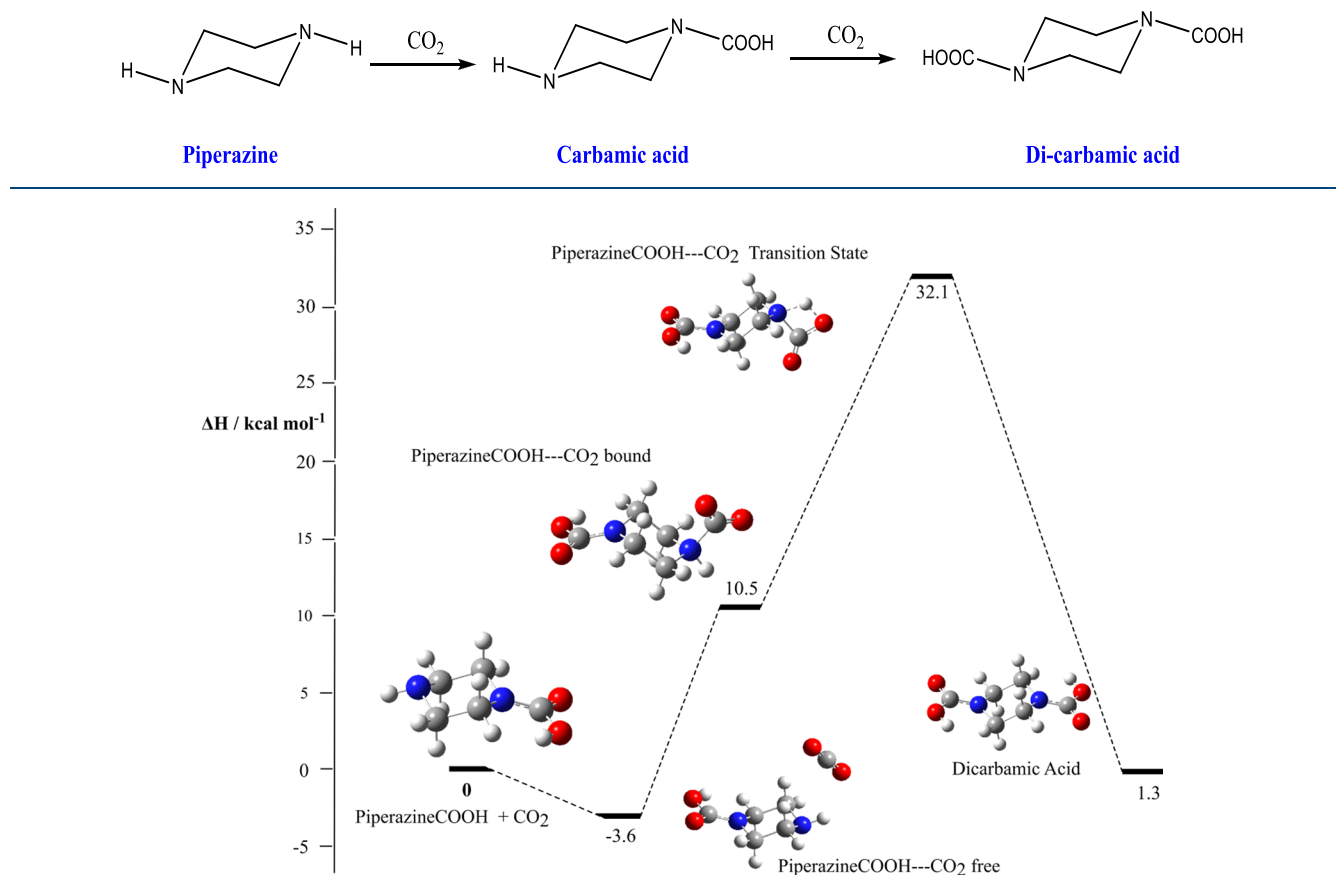
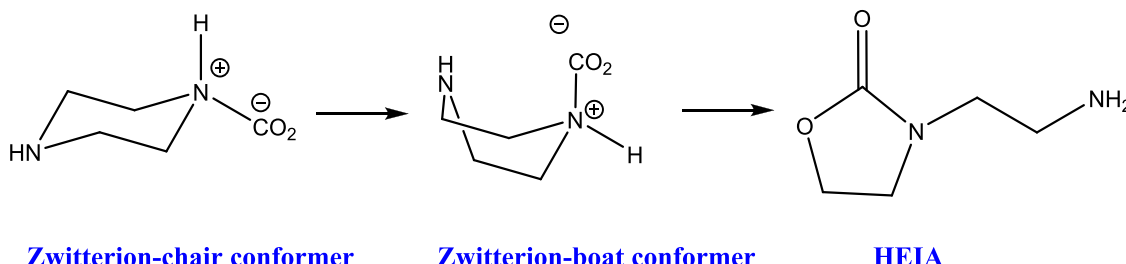
### 3. RESULTS AND DISCUSSION

**3.1. Reactions with  $\text{CO}_2$  (Carbonate, Ion Pair, Carbamic Acid, and Dicarbamic Acids).** Piperazine can exist in solution in a number of low-energy chair conformers as illustrated in Scheme 1 (eq, eq. ax, eq. ax, ax). They differ in the orientation of the N–H bond, which can be either in the axial or equatorial position. The relative enthalpies of these conformers were calculated to be 0.0, 0.08, and 0.45 kcal mol<sup>-1</sup>, respectively. While a thorough investigation of the implications of these conformers on each reaction is beyond the scope of this work, it is presented to illustrate that they are thermally accessible and

may aid in rationalizing some of the more complex mechanisms postulated here.

Piperazine contains two amine groups and consequently can react with up to two molecules of  $\text{CO}_2$ . Initial binding of  $\text{CO}_2$  to one amine group leads to a zwitterionic complex with a positive charge on the nitrogen and a negative charge on the carboxylate group. This species can react either intramolecularly or intermolecularly (assisted by hydrogen transfer to and from a water molecule) to form a carbamic acid. Alternatively, it can react with another molecule of piperazine to form an ion pair complex. These reactions are summarized in Scheme 2.

The DFT-calculated energy profile for the reactions presented in Scheme 2 is shown in Figure 2. Formation of the ion pair is very favorable with an activation energy of only 2.4 kcal mol<sup>-1</sup>. In contrast, carbamic acid formation is less likely with an activation energy of 33.8 kcal mol<sup>-1</sup>. This value can be reduced significantly to 11.6 kcal mol<sup>-1</sup> if the hydrogen transfer is intermolecular rather than intramolecular. Given the relative concentration of piperazine in the reaction mixture, it is more likely that formation of the ion pair dominates compared to carbamic acid formation. However, if the  $\text{CO}_2$  loadings are particularly high, then carbamic acid formation could still be favored.

**Scheme 3.** Formation of a Dicarbamic Acid from the Reaction of CO<sub>2</sub> and Piperazine**Figure 3.** DFT-calculated  $\Delta H$  energy profile for the proposed formation of a dicarbamic acid from PiperazineCOOH.**Scheme 4.** Potential Route to the Formation of HEIA via Cyclization from a Piperazine Zwitterion Complex

As mentioned previously, piperazine can react with up to two molecules of CO<sub>2</sub> and can potentially form a dicarbamic acid. Scheme 3 summarizes the reaction.

The energy profile for the formation of dicarbamic acid starting from carbamic acid is shown in Figure 3. Formation of the prereaction complex (labeled PiperazineCOOH-CO<sub>2</sub> free in Figure 3) is favorable. Binding of the CO<sub>2</sub> molecule to the free amine nitrogen is endoergic (14.1 kcal mol<sup>-1</sup>). The activation energy for the formation of dicarbamic acid is 35.7 kcal mol<sup>-1</sup> and can be reduced by hydrogen transfer to and from a water molecule as shown previously. Given the standard experimental temperatures, formation of a dicarbamic acid is feasible.

**3.2. Cyclization from Boat Structure to Form HEIA.** The initial degradation products of MEA result from cyclization of either the ion pair species or carbamic acid to form oxazolidinone. Such products are not observed during piperazine degradation, so this was next investigated. The

nucleophilic oxygen on the carboxylate group can potentially react with a carbon atom  $\alpha$  to the amine nitrogen in the 4 position. For this to proceed, the amine species needs to be in a boat conformation rather than chair. In the chair conformation, the two reactive sites are too far away for a reaction to occur. This process is summarized in Scheme 4.

The energy profile for the formation of HEIA is shown in Figure 4. Rearrangement to the appropriate boat conformer carries an energy penalty of 14.6 kcal mol<sup>-1</sup>. The activation energy for HEIA formation is prohibitively high (101.9 kcal mol<sup>-1</sup>). Moreover, the reaction energy is also significantly endothermic. Given these observations, HEIA will not form from the zwitterionic species *via* this route as is consistent with experimental observations.

### 3.3. Thermal Degradation Products of Piperazine.

**3.3.1. Hydrolysis of Piperazine.** The thermal degradation of piperazine is considered to be dominated by nucleophilic

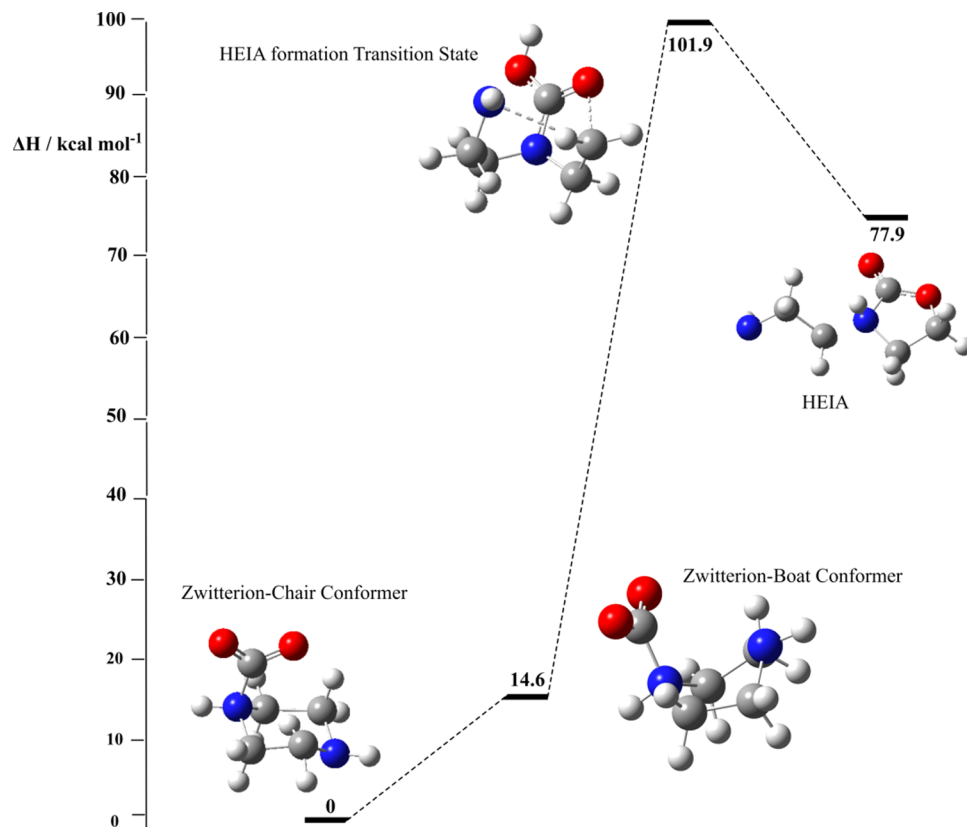
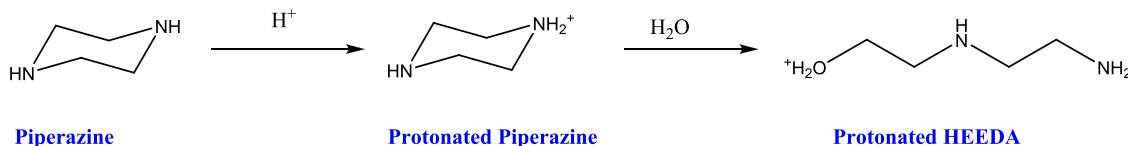


**Figure 4.** DFT-calculated  $\Delta H$  energy profile for the proposed formation of HEIA from a zwitterion.

**Scheme 5. Potential Route to the Formation of HEEDA via the Hydrolysis of Piperazine**



substitution reactions and has been observed in other amine systems.<sup>39</sup> Protonation of the amine nitrogen creates a much better leaving group. This increases the susceptibility of the protonated amine to undergo a substitution reaction. Attack of a nucleophilic nitrogen at either of the carbon atoms  $\alpha$  to the protonated amine group yields the product complex.

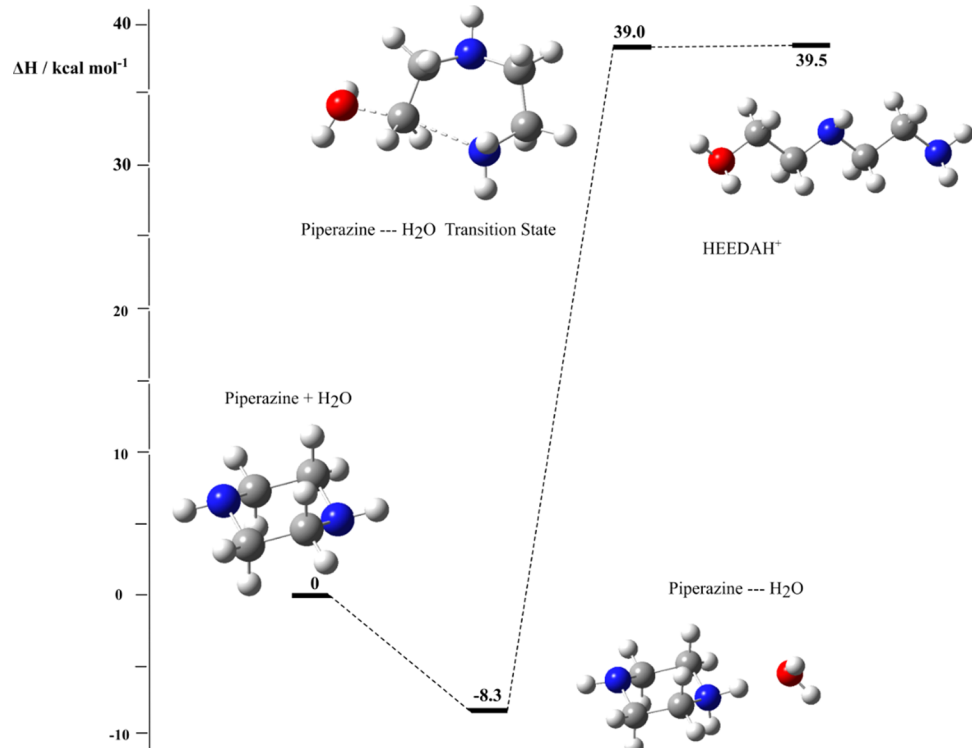
Our first consideration was given to whether piperazine could undergo a hydrolysis reaction at high temperatures to form a linear amine species as in Scheme 5. The calculated energy profile is shown in Figure 5. As expected, the initial interaction between the protonated piperazine and water is favorable. The activation energy is 47.3 kcal mol<sup>-1</sup> and the reaction is overall endoergic. This would suggest that piperazine is resistant to hydrolysis even at elevated temperatures.

**3.3.2. Formation of AEAEPZ, AEAEPZ-UREA, N-(2-Hydroxyethyl)piperazine (HEP), and 1,1'-(1,2-Ethandiyil)bipiperazine (PEP).** Given that the concentration of piperazine will initially be high, the first observed degradation products are likely to arise from a reaction between piperazine and protonated piperazine ( $PipH^+$ ). This reaction is summarized in Scheme 6. The nitrogen atom of piperazine acts as a nucleophile and reacts with an electrophilic carbon atom  $\alpha$  to the protonated nitrogen of  $PipH^+$ . This causes the ring of  $PipH^+$  to open and forms protonated AEAEPZ.

Figure 6 shows the energy profile for the formation of AEAEPZ from piperazine and  $PipH^+$ . There is a favorable interaction between the two reactants in the pre-collision complex (defined as the structure immediately preceding the transition state where the reactants are in close proximity). The activation energy is 23.9 kcal mol<sup>-1</sup>. Given the experimental temperatures of 100–150 °C, this route is feasible and is likely to be the route to the first observed degradation product.

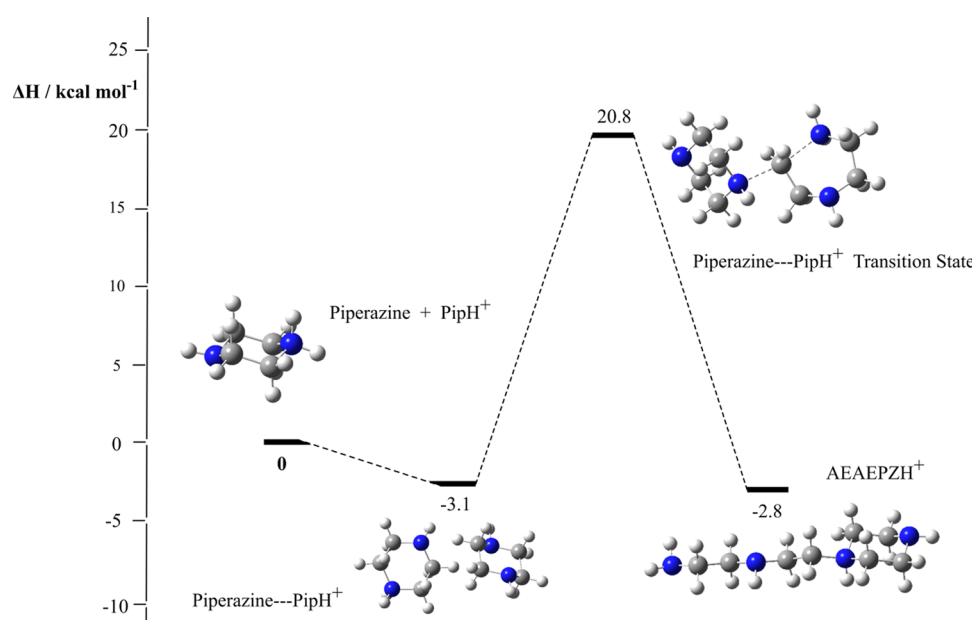
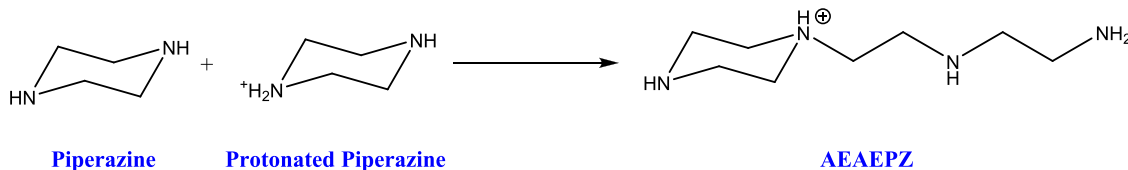
Once formed, the protonated AEAEPZ can potentially react with any other amine species present in the reaction medium. Given the number of species that could be potentially involved, we have not investigated any polymeric products. Instead, the reactions with both piperazine and CO<sub>2</sub> were considered as these two reactants are still likely to be present in large quantities in the early stages of degradation. As shown in Scheme 7, CO<sub>2</sub> can bind to either of the nitrogen atoms in the pendant chain. A ring-closing reaction can then form a urea species. (The reaction of CO<sub>2</sub> at the ring nitrogen in AEAEPZ was not considered as the species formed cannot form AEAEPZ-UREA.)

The energy profile for the formation of AEAEPZ-UREA is shown in Figure 7. Initial binding of CO<sub>2</sub> to the amine requires 9.3 kcal mol<sup>-1</sup>. The activation energy to form carbamic acid is 33.4 kcal mol<sup>-1</sup>. This value can likely be reduced significantly by proceeding through an intermolecular reaction with water as demonstrated previously. The activation energy for ring



**Figure 5.** DFT-calculated  $\Delta H$  energy profile for the proposed hydrolysis of piperazine.

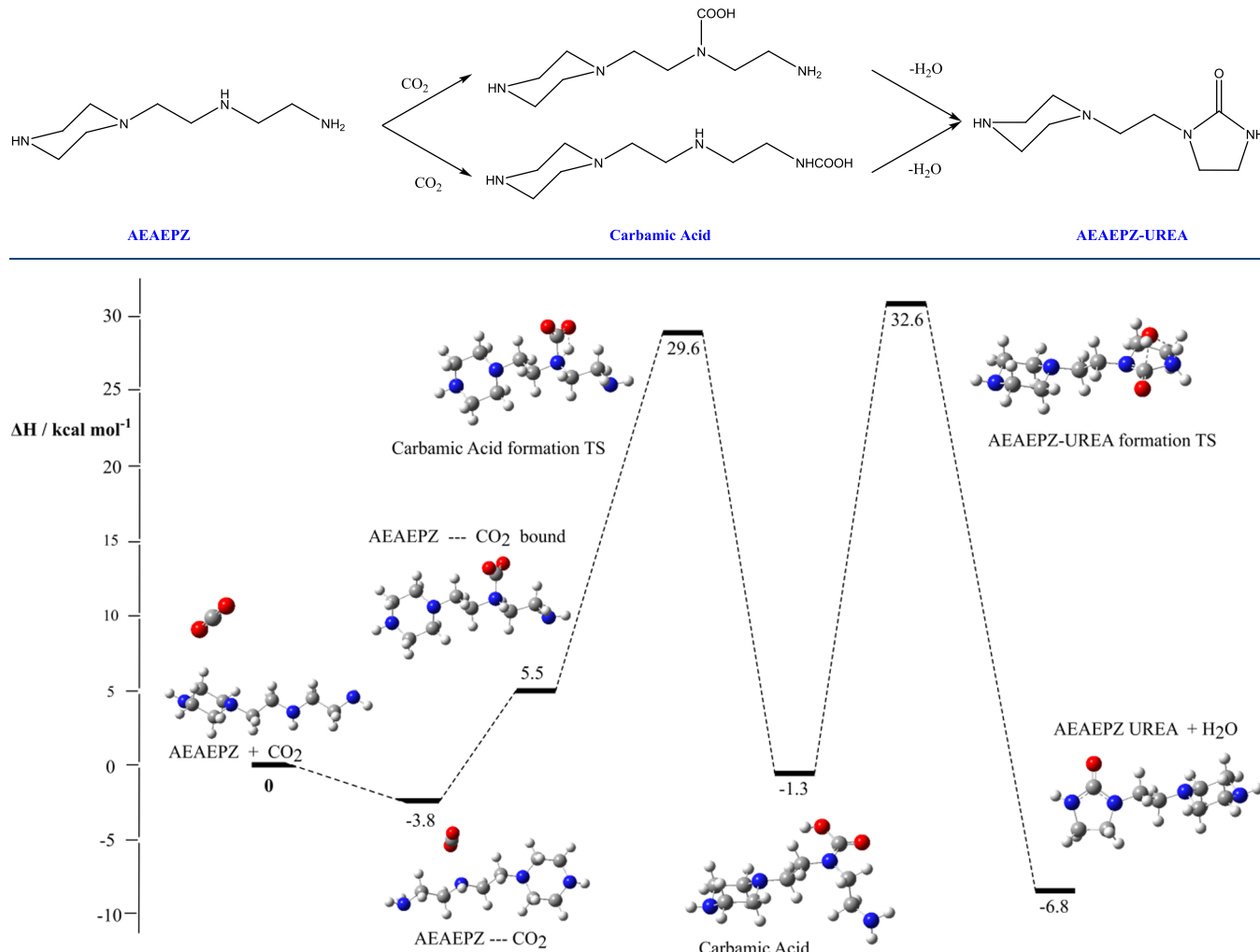
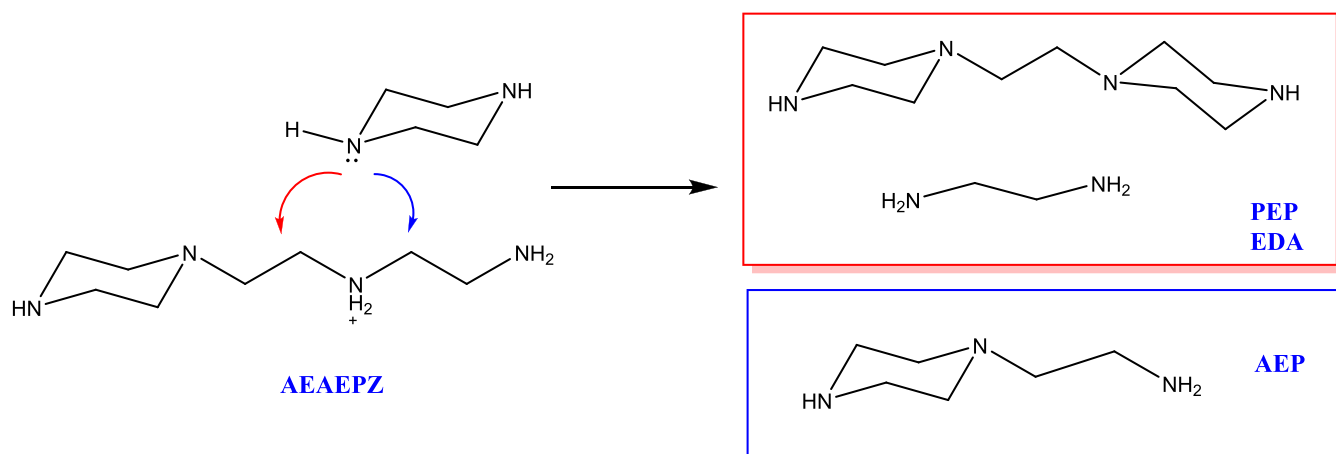
**Scheme 6. Potential Route to the Formation of AEAEPZ from the Reaction between Piperazine and PipH<sup>+</sup>**



**Figure 6.** DFT-calculated  $\Delta H$  energy profile for the proposed formation of AEAEPZ from the reaction between piperazine and PipH<sup>+</sup>.

formation is calculated to be 33.9 kcal mol<sup>-1</sup>. This reaction also expels water.

Protonation of AEAEPZ can occur at any of the nitrogen atoms. Reaction with piperazine can lead to two sets of products

**Scheme 7.** Formation of AEAEPZ-UREA from the Reaction of AEAEPZ and CO<sub>2</sub>**Figure 7.** DFT-calculated ΔH energy profile for the proposed formation of AEAEPZ-UREA from AEAEPZ and CO<sub>2</sub>.**Scheme 8.** Formation of Either PEP and EDA or AEP via the Reaction of Piperazine and AEAEPZ

if a nitrogen on the linear chain is protonated as shown in **Scheme 8**. If nucleophilic substitution occurs at the α carbon to the protonation site furthest from the ring, then there are two equivalents of *N*-(2-aminoethyl)piperazine (AEP) for every reaction (blue pathway in **Scheme 8**). Alternatively, if the attack at the other α carbon is favored, this leads to the formation of

PEP and EDA (red pathway in **Scheme 8**). The energy profile for both reactions is shown in **Figure 8**.

The prereaction complex is more stable than the separated reactants by 15.0 kcal mol<sup>-1</sup>. The activation energies are 33.7 and 33.4 kcal mol<sup>-1</sup> for the formation of PEP-EDA and AEP-AEP, respectively. This illustrates that attack at either carbon

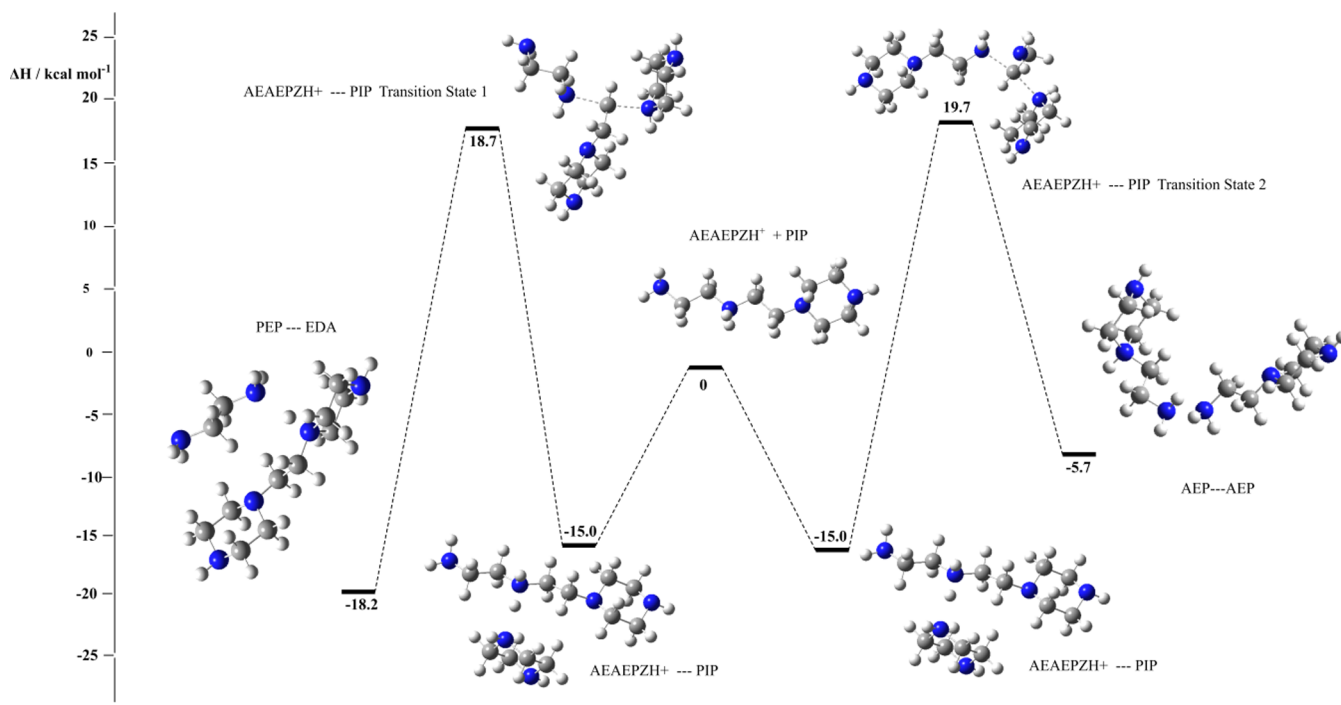
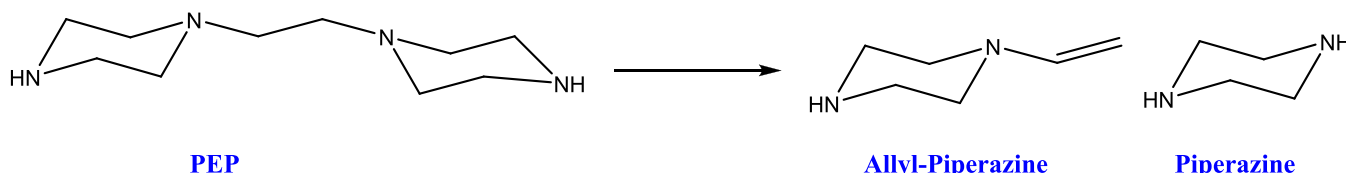
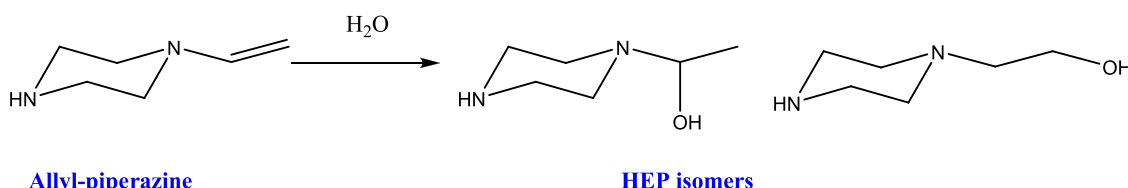


**Figure 8.** DFT-calculated  $\Delta H$  energy profile for the nucleophilic attack of piperazine on protonated AEAEPZ leading to two sets of products.

**Scheme 9. Thermal Decomposition of PEP**



**Scheme 10.** Reaction of Allyl-Piperazine with H<sub>2</sub>O to Form Two Isomeric Products of HEP



atom is as likely as the other. Given that the relative steric bulk and partial charge at each site is very similar, this result is expected. While these activation barriers are high for each substitution reaction, they are not insurmountable, given the standard experimental conditions.

With sufficient heating, PEP can fragment to form allyl-PEP and piperazine as shown in Scheme 9.

As shown in **Scheme 10**, any allyl-piperazine that is generated can subsequently be hydrolyzed. The DFT-calculated energy profile for the reaction of allyl-piperazine and water is shown in **Figure 9**. The reaction to form secondary HEP, where the hydroxyl group is on the carbon directly bonded to the amine, is significantly favored compared to formation of primary-HEP. This is rationalized via analysis of the transition states. A carbocation is formed in the transition state leading to the formation of both products. In the secondary-HEP formation transition state, the carbocation is placed on the carbon directly bound to the amine. This is stabilized by interactions with the p-orbital on the nitrogen. In comparison, the primary carbocation

formed in the alternative transition state does not benefit from this stability.

**3.3.3. Formation of 1, 2-Ethanediamine, N1-(2-Aminoethyl) (DETA), AEP, 1, 4-Diazabicyclo[2.2.2]octane (TEDA), and Imidazolidinone.** As shown in Section 3.3.2, EDA can be formed from the reaction of AEAEPZ and piperazine. If the concentration of EDA builds up in the reaction media, then it can potentially undergo a series of similar reactions to those presented earlier for piperazine, namely, binding with CO<sub>2</sub> and subsequently forming either an ion pair or carbamic acid. Furthermore, these species can cyclize to form imidazolidinones, which have been observed experimentally.<sup>14</sup> Reactions with piperazine are also presented and are more likely than reactions with other imines whose concentrations are still likely to be significantly lower than piperazine. The various reactions of EDA and CO<sub>2</sub> are summarized in Scheme 11.

The energy profile in Figure 10 shows that formation of an ion pair is more favorable than carbamic acid formation as was observed for piperazine in Section 3.1. However, the formation

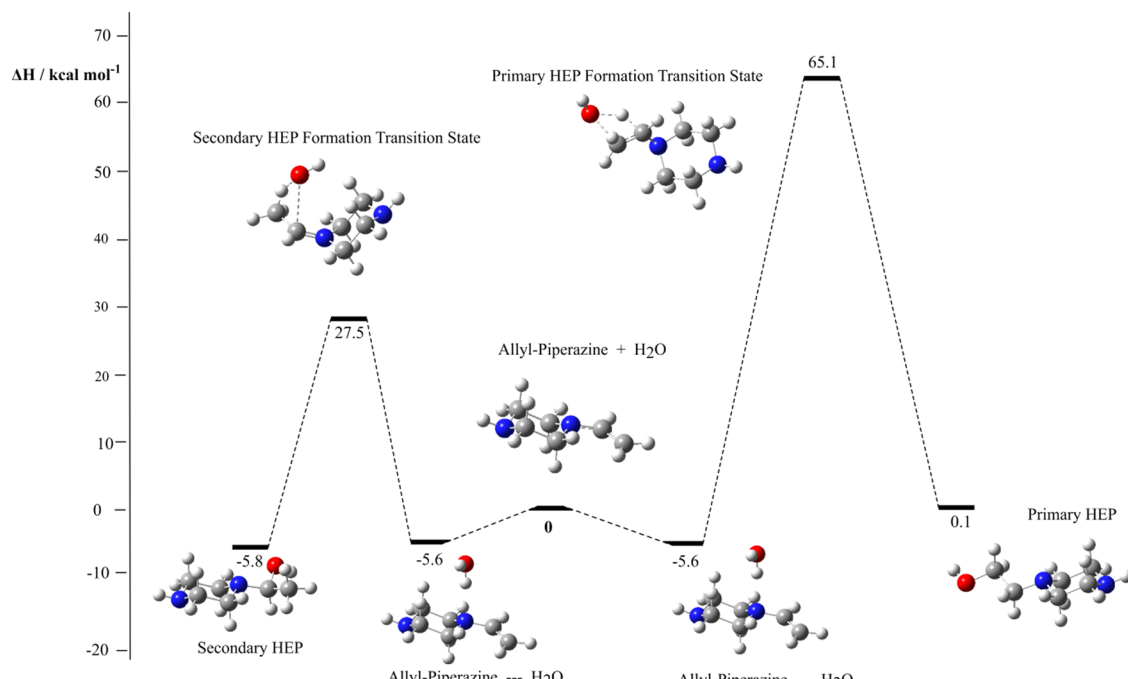
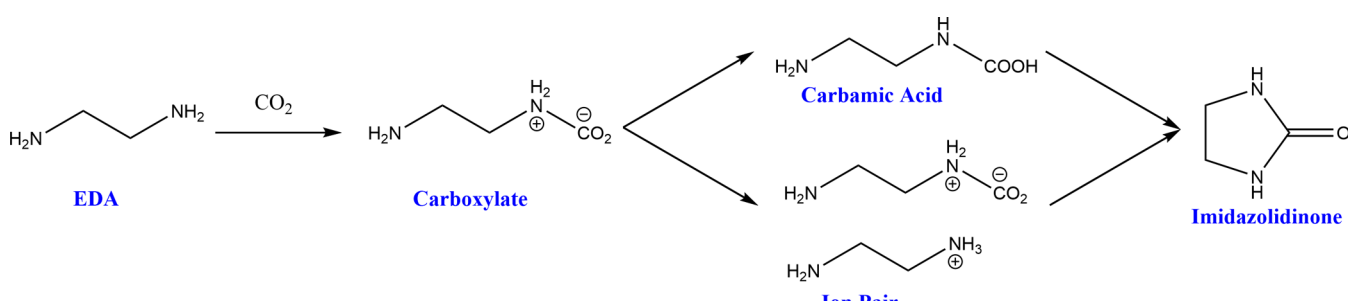


**Figure 9.** DFT-calculated  $\Delta H$  energy profile for the proposed formation of two isomers of HEP from allyl-piperazine.

**Scheme 11. Suggested Formation of Both Carbamic Acid and an Ion Pair Species from EDA and Subsequent Cyclization to Form Imidazolidinone**



of carbamic acid can be made more favorable by an intermolecular reaction with water as demonstrated previously. Given that EDA is postulated to form from the reaction of piperazine and AEAEPZ, which itself is formed from the reaction of piperazine and PIPH<sup>+</sup>, the relative concentration of EDA is likely to be comparatively low. Thus, the reaction with CO<sub>2</sub> is more likely than the formation of an ion pair via the reaction of two EDA molecules.

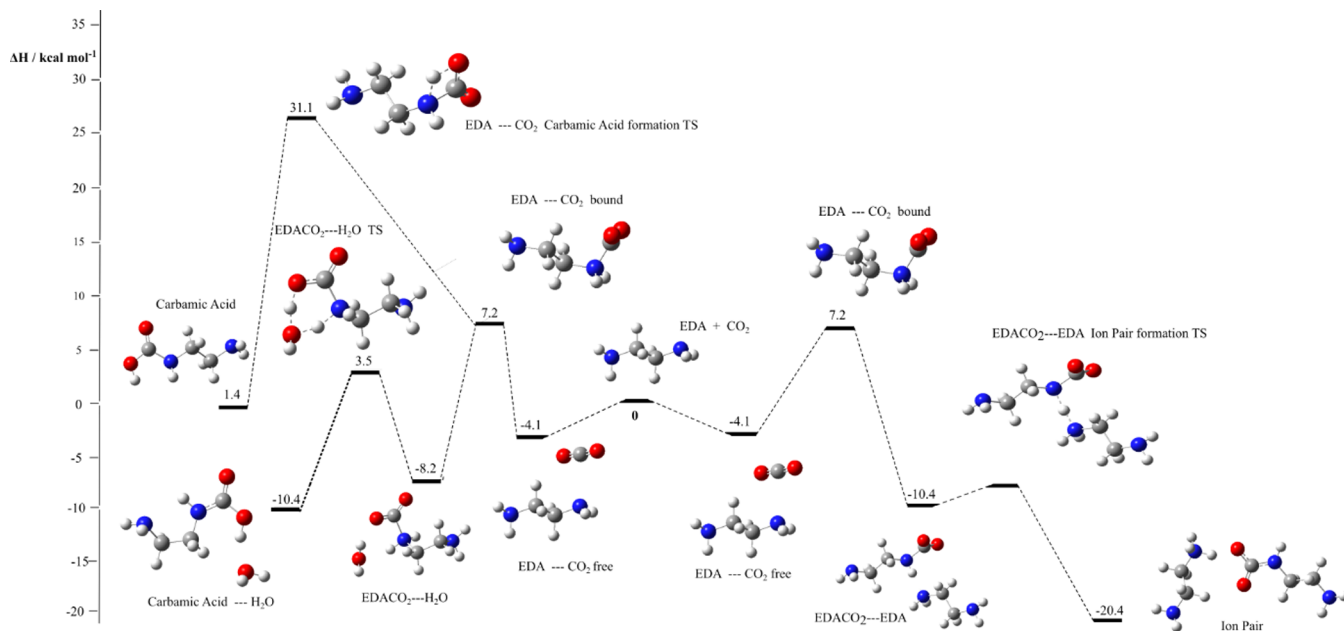
Next, we investigated the cyclization reaction of the carbamic acid to form imidazolidinone as shown in Scheme 12. The nitrogen atom of the amine can act as a nucleophile and attacks the carbonyl carbon of the acid group. In turn, this reaction eliminates water and forms imidazolidinone. The energy profile is shown in Figure 11.

The intermolecular reaction of AEP can lead to the formation of TEDA as in Scheme 13. For the reaction to proceed, a geometry change is necessary. As was observed for the potential formation of HEIA, the reactant needs to be in a boat conformer with the pendant chain angled in such a way as to bring the reactive sites into close proximity. The energy profile for the reaction is shown in Figure 12. Overall, the conformational change carries an energy penalty of 10.1 kcal mol<sup>-1</sup>. Protonation of the pendant primary amine to afford a better

leaving group is very favorable. The protonated boat conformer can then react intramolecularly to eliminate ammonia and form protonated TEDA. The activation energy for this reaction is 18.5 kcal mol<sup>-1</sup> and the reaction is thermodynamically favorable.

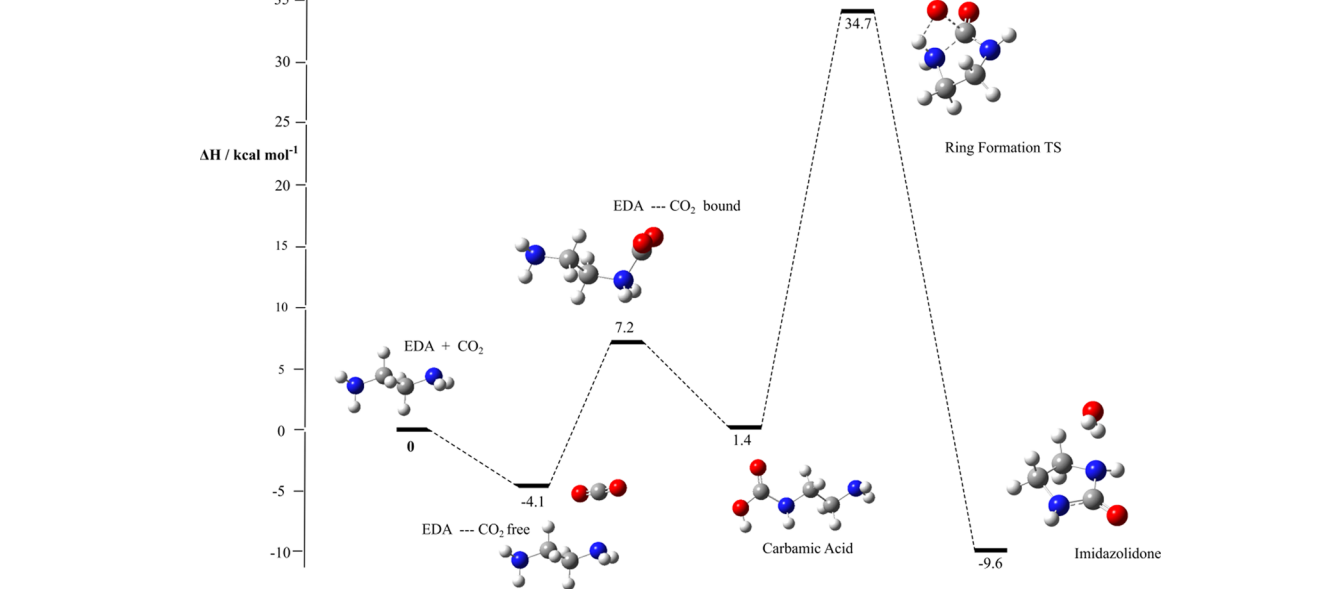
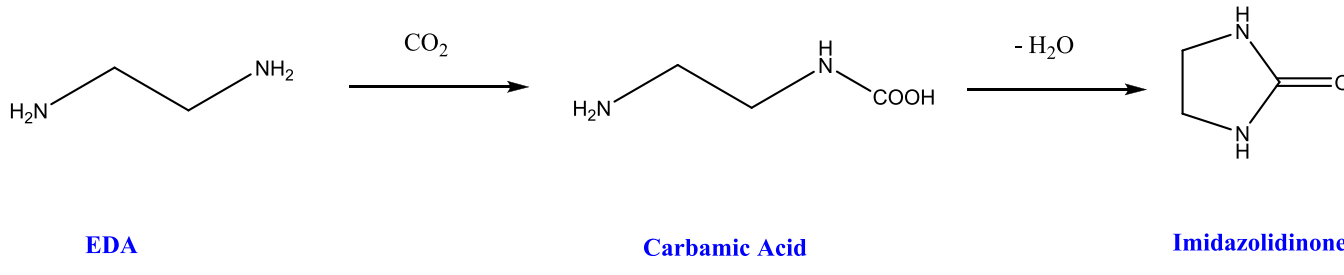
**3.3.4. 1-(2-Aminoethyl)-2-imidazolidinone (AEI) from Imidazolidinone and DETA.** AEI is a substituted imidazolidinone whose formation can be rationalized by two routes as shown in Scheme 14. CO<sub>2</sub> can bind to any of the nitrogen atoms on DETA, which itself is formed from the reaction of two EDA molecules and through subsequent cyclization can form AEI via the elimination of water. Alternatively, a nucleophilic substitution reaction between an imidazolidinone and EDA can yield the target product.

The energy profiles for AEI formation from DETA and imidazolidinone are shown in Figures 13 and 14, respectively. The activation energy for cyclization is 33.7 kcal mol<sup>-1</sup> and the reaction is exothermic. In contrast, the formation from imidazolidinone and EDAH<sup>+</sup> has a higher activation energy (35.8 kcal mol<sup>-1</sup>) and the reaction is endothermic. While these observations do not preclude the possibility of formation from an imidazolidinone, it is much more likely that AEI forms from the reaction of DETA and CO<sub>2</sub>.



**Figure 10.** DFT-calculated  $\Delta H$  energy profile for the proposed formation of carbamic acid and an ion pair from EDA and  $\text{CO}_2$ .

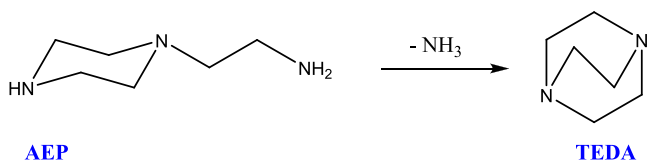
**Scheme 12. Formation of Imidazolidinone from EDA and  $\text{CO}_2$**



**Figure 11.** DFT-calculated  $\Delta H$  energy profile for the proposed formation of imidazolidinone from EDA and  $\text{CO}_2$ .

**3.4. Oxidative Degradation. 3.4.1. Piperazine Fragmentation and Subsequent Reactions with Oxygen.** Oxidative degradation of the amine solvent occurs mainly in the stripper.<sup>40,41</sup> While the specific mechanisms are still being

debated, it is considered to be initiated by the presence of free radical species such as oxygen,  $\text{OH}$ , and/or trace metals (e.g.,  $\text{Fe}^{2+}$ ,  $\text{Cr}^{3+}$ ,  $\text{Ni}^{2+}$ , and  $\text{Mn}^{2+}$ ). There are two potential hydrogen abstraction sites on piperazine, namely, the NH and the ring

**Scheme 13.** Proposed Formation of TEDA from AEP

hydrogen atoms, which are all equivalent, as illustrated in **Scheme 15**. Abstraction of ring hydrogen and subsequent radical recombination reactions form a hydroperoxide species. Hydroperoxides can thermally decompose to form two radical species (normally a peroxy and a hydroxy radical). Further radical abstractions can lead to the formation of OPZ.

The energy profile for the reaction of OH and piperazine is shown in **Figure 15**. The most kinetically viable reaction is abstraction of the NH hydrogen. This reaction has an activation energy of  $1.7 \text{ kcal mol}^{-1}$  compared to  $8.2 \text{ kcal mol}^{-1}$  for abstraction of a hydrogen from a CH bond. Given that the N–H bond strength is weaker than C–H, this result is expected and consistent with other literature studies.<sup>42</sup>

Once formed, the piperazine radical species can recombine with oxygen and a further radical source to form a hydroperoxide species. Thermal fission of this species to form two oxygen-centered radicals requires  $34.3 \text{ kcal mol}^{-1}$  and is comparable with reported values. **Figure 16** shows how the generated species with a radical on the ring oxygen can react with an OH radical to form OPZ. The OH radical abstracts a hydrogen atom from the ring to generate OPZ and  $\text{H}_2\text{O}$ . This reaction is thermodynamically very favorable and has a low kinetic barrier ( $12 \text{ kcal mol}^{-1}$ ).

**3.4.2. EDA Fragmentation.** A route to the formation of EDA was presented in **Section 3.4.1**. EDA can undergo similar radical reactions to those shown for piperazine. Similarly, there are two potential hydrogen abstraction sites on EDA as illustrated in **Scheme 16**, namely, the  $-\text{CH}_2$  groups and the amine groups. On forming, the radical species can subsequently fragment into smaller amines and imines.

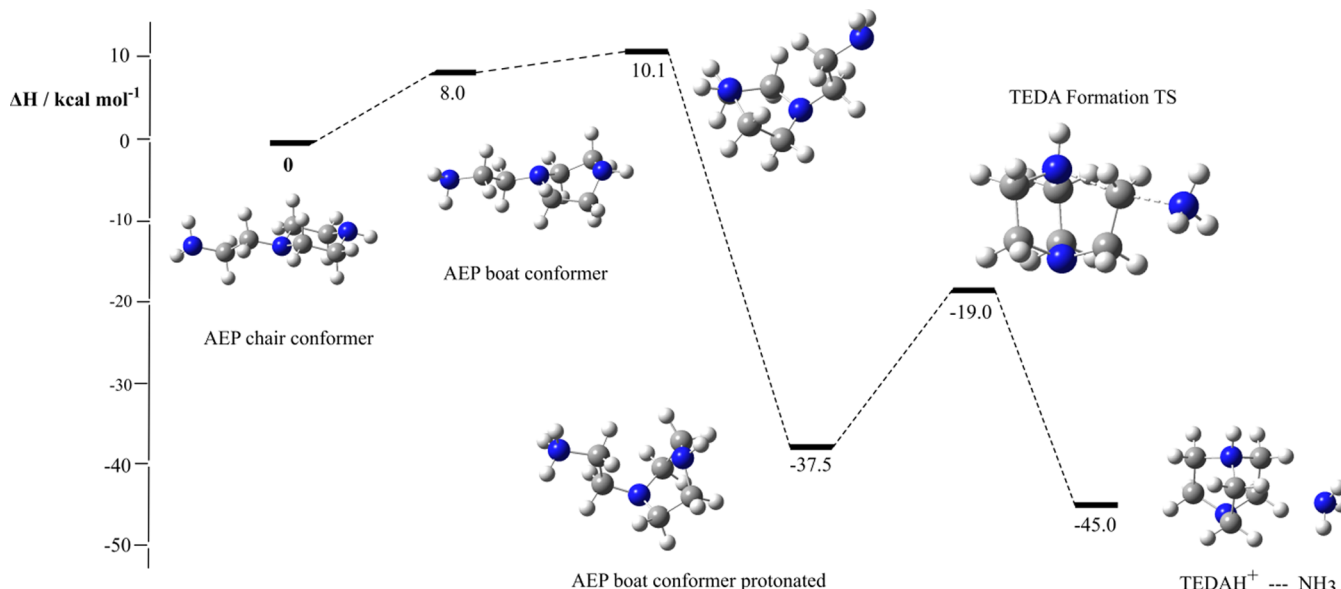
The DFT-calculated energy profile is shown in **Figure 17**. As observed for the reaction of piperazine and OH, abstraction of a

hydrogen from the N–H bond on EDA is more favorable than from C–H ( $1.9 \text{ cf. } 3.8 \text{ kcal mol}^{-1}$ ). Despite this, both reactions are kinetically and thermodynamically favorable given the experimental conditions.

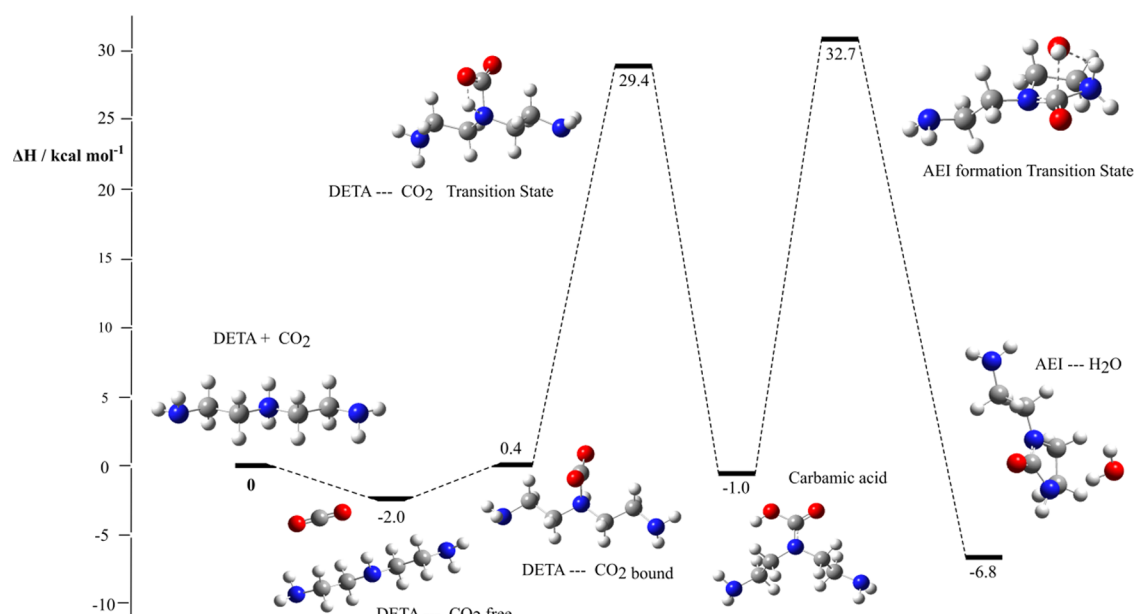
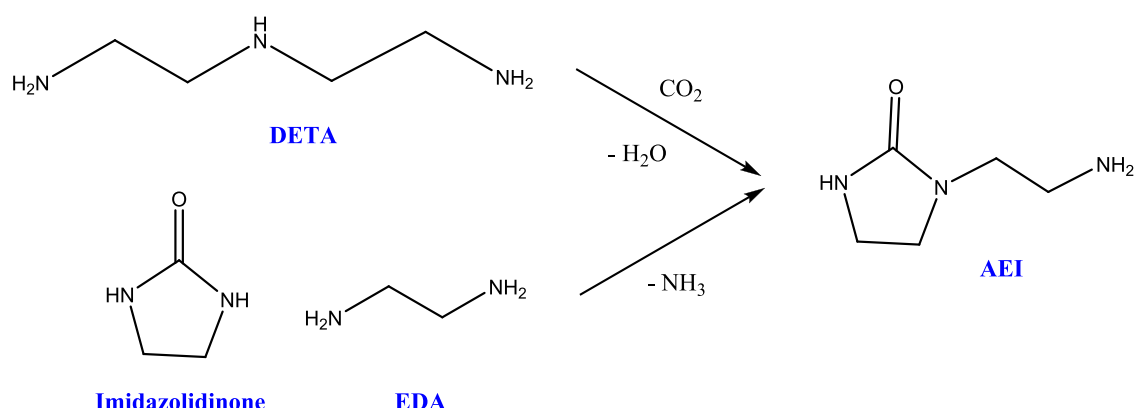
We recently reported on the fragmentation reactions that MEA radicals can occur, which were shown to thermally decompose to form amines, water, and imines. Here, a similar set of reactions can be envisaged for EDA radicals. **Scheme 16** shows how the radical species might fragment to form ammonia, methylamine, and two further imine species.

The DFT-calculated energy profiles for fragmentation of both radical species are shown in **Figure 18**. As can be seen, the species with the radical located on nitrogen has a lower activation barrier to fragmentation compared to that located on the carbon. However, the reaction is endothermic, most likely due to the instability of the methylamine radical species generated. Subsequent more favorable reactions would likely be needed to drive the reaction forward and prevent rapid recombination. In contrast, fragmentation of the species with the radical located on the carbon atom is exothermic overall, the reaction being driven by formation of a more stable radical species.

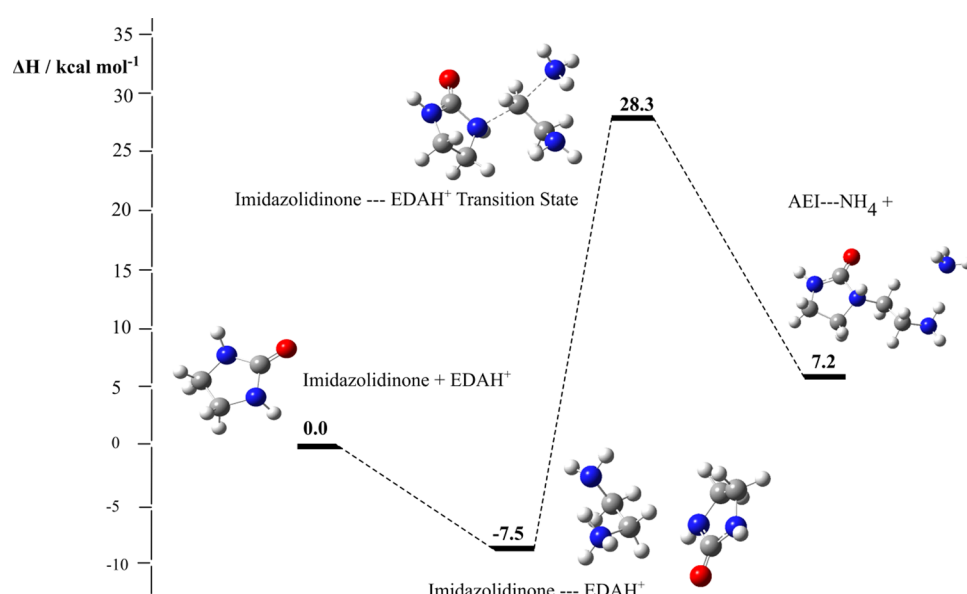
**3.4.3. EDACO<sub>2</sub>H Fragmentation to Form Formate.** Freeman et al. observed that when degradation studies were performed using <sup>13</sup>C-labeled CO<sub>2</sub>, the label was subsequently present in formate and formic acid at the end of the study.<sup>14</sup> This observation would require a mechanism where the formate is solely produced from the free CO<sub>2</sub> and not through degradation of any other species. **Scheme 17** shows potential route to the formation of formic acid, starting with a carbamic acid formed from EDA. As can be seen in **Figure 19**, the abstraction of a hydrogen from the central chain is both kinetically and thermodynamically favorable. This forms a radical species, which can potentially fragment to form formic acid. However, despite this fragmentation reaction being thermodynamically viable, it has a high kinetic barrier ( $37.5 \text{ kcal mol}^{-1}$ ). While this barrier may be surmountable given the elevated temperature and pressure experienced in the stripper, it is more likely that another

**Figure 12.** DFT-calculated  $\Delta H$  energy profile for the proposed formation of TEDA from AEP.

**Scheme 14.** Two Alternative Routes to the Formation of AEI from either the Cyclization Reaction of DETA and CO<sub>2</sub> or Nucleophilic Substitution of EDA and an Imidazolidinone

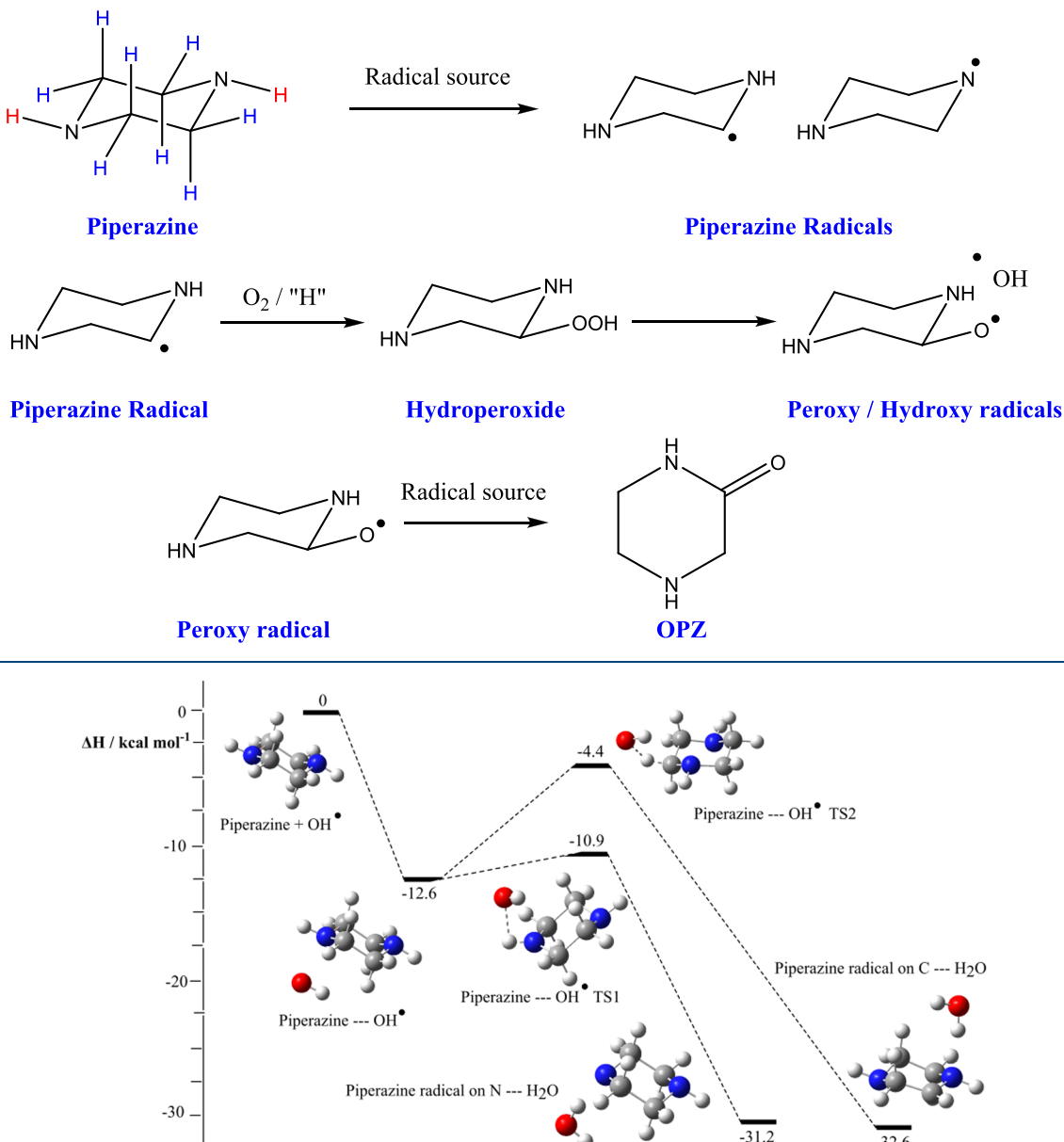


**Figure 13.** DFT-calculated  $\Delta H$  energy profile for the proposed formation of AEI from DETA and CO<sub>2</sub>.



**Figure 14.** DFT-calculated  $\Delta H$  energy profile for the proposed formation of AEI from imidazolidinone and EDAH<sup>+</sup>.

Scheme 15. Radical Reactions with Piperazine Leading to the Formation of OPZ

Figure 15. DFT-calculated  $\Delta H$  energy profile for the reaction of piperazine and OH radical.

mechanism is responsible for the production of formic acid. Further work would be required to identify this mechanism.

**3.4.4. MPZ Formation from Piperazine.** The final degradation product that was investigated was MPZ. Scheme 18 shows how this can be formed from the reaction of piperazine and protonated methylamine, which itself is a product of EDA radical fragmentation. Figure 20 shows the DFT-calculated energy profile for the reaction, which is predicted to be kinetically and thermodynamically viable.

**3.5. Nitrosamine Formation.** Nitramines and nitrosamines can be formed in carbon-capture plants as a result of nitrogen oxides ( $\text{NO}_x$ ) reacting with amines (mainly secondary amines; primary amines do not form stable nitrosamines). The environmental impact of their release into the atmosphere represents a major concern. Hence, a significant amount of experimental research has been conducted to verify the mechanism of formation.<sup>43–47</sup>

Here, we investigated the formation of these species via the reaction of an amine with  $\text{N}_2\text{O}_3$ . As shown in Scheme 19, there are two primary routes to the formation of the nitrosamine product. The amine can act as a nucleophile and attack the “NO” group of  $\text{N}_2\text{O}_3$ . This eliminates  $\text{NO}_2^-$  and creates an ion pair. Subsequent nucleophilic attack of  $\text{NO}_2^-$  on the N–H forms nitrous acid and a nitrosamine. Alternatively, a concerted reaction can occur, which involves rearrangement of multiple atoms at once to form the same products.

Despite multiple attempts, a transition state corresponding to the first pathway could not be located. Figure 21 shows the energy profile for the formation of a nitrosamine from  $\text{N}_2\text{O}_3$ . The activation energy is very low (7.2 kcal mol<sup>-1</sup>) and the reaction energy is also exothermic, suggesting that nitrosamine formation should be very facile.

We carried out similar modeling studies for nitrosamine formation from AEI, AEP, imidazolidinone, HEP, and AEAEPZ,

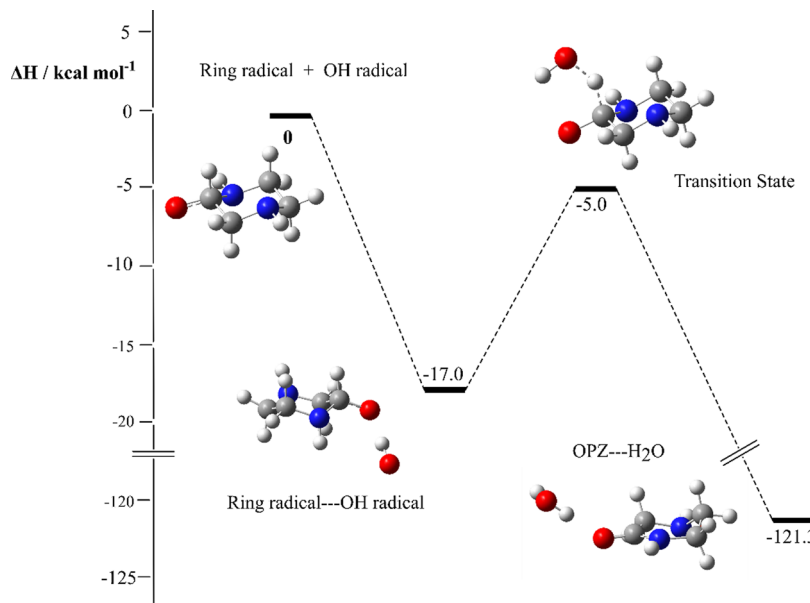


**Figure 16.** DFT-calculated  $\Delta H$  energy profile for the formation of OPZ.

**Scheme 16. EDA Radical Formation and Subsequent Fragmentation Leading to the Production of Smaller Amines and Imines**

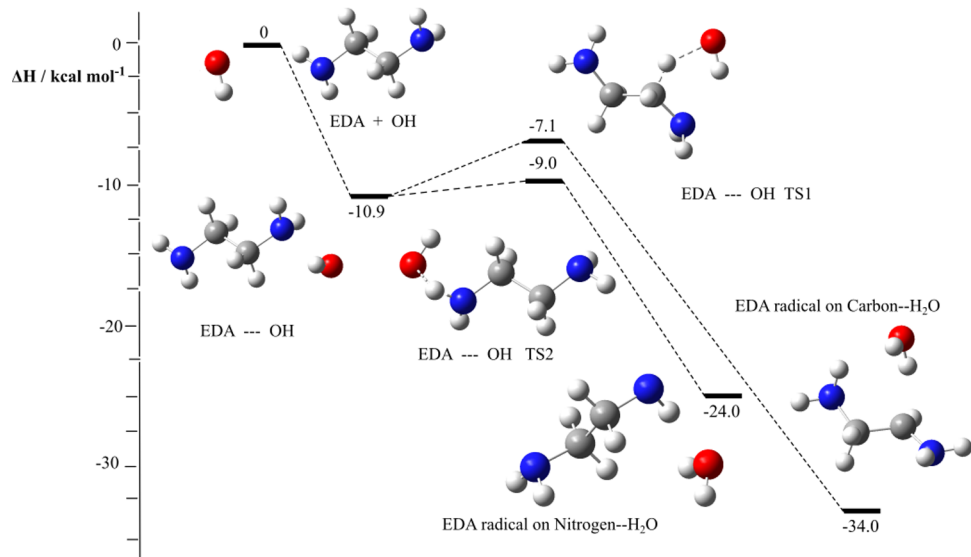
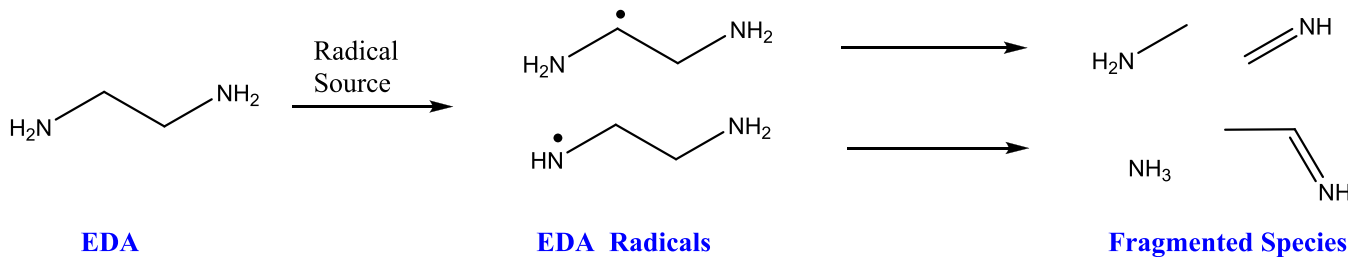


**Figure 17.** DFT-calculated  $\Delta H$  energy profile for the reaction of EDA and OH radical.

the results of which are tabulated in **Table 1**. For AEI and AEP, two reaction sites were investigated. For the case of AEAEPZ, three sites were probed. As observed for imidazolidinone, the activation energies for nitrosamine formation are very low for all amine species ( $0.67\text{--}7.21\text{ kcal mol}^{-1}$ ). Similar results were reported by Shi et al.<sup>48</sup>

**3.6. Schematic Reaction Network.** **Figure 22** shows a schematic network summarizing the major findings of this work. Initially, piperazine can react with  $\text{CO}_2$  to form various carboxylates and carboxylic acids (both mono- and di-substituted). Alternatively, piperazine can undergo a series of nucleophilic substitution reactions, aided by protonation, to form larger substituted amines. Fragmentation reactions, most

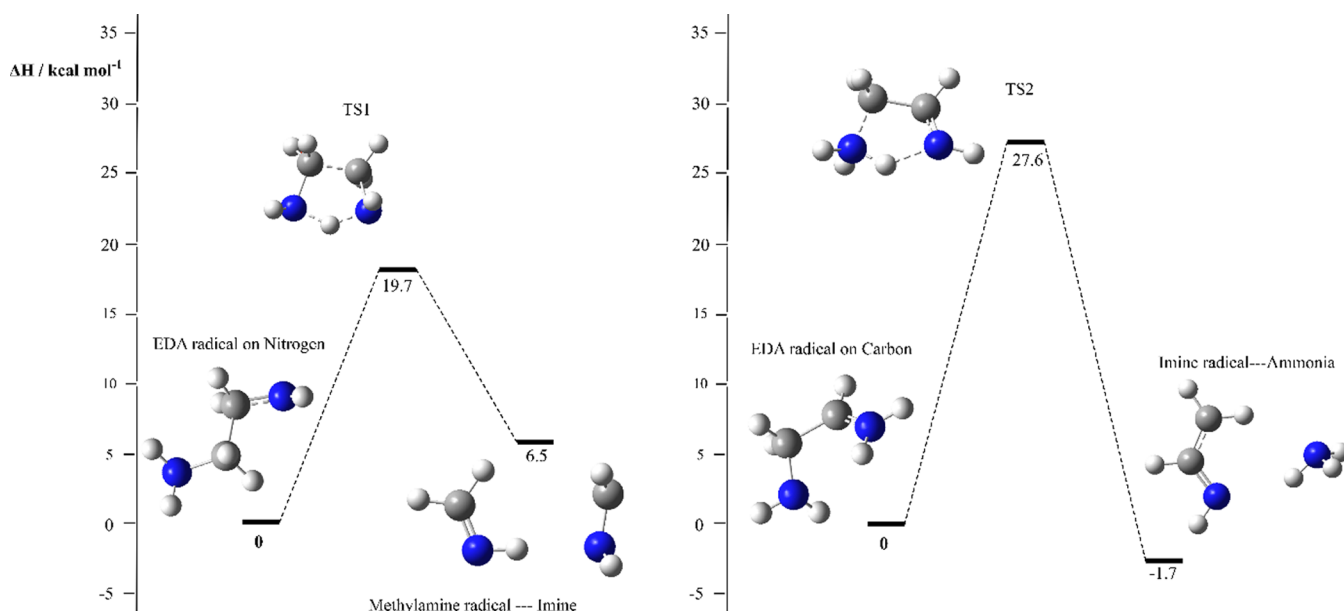


**Figure 18.** DFT-calculated  $\Delta H$  energy profiles for fragmentation of EDA radicals located on nitrogen (left) and carbon (right).

**Scheme 17. Proposed Radical Formation and Subsequent Fragmentation to Form Formic Acid**

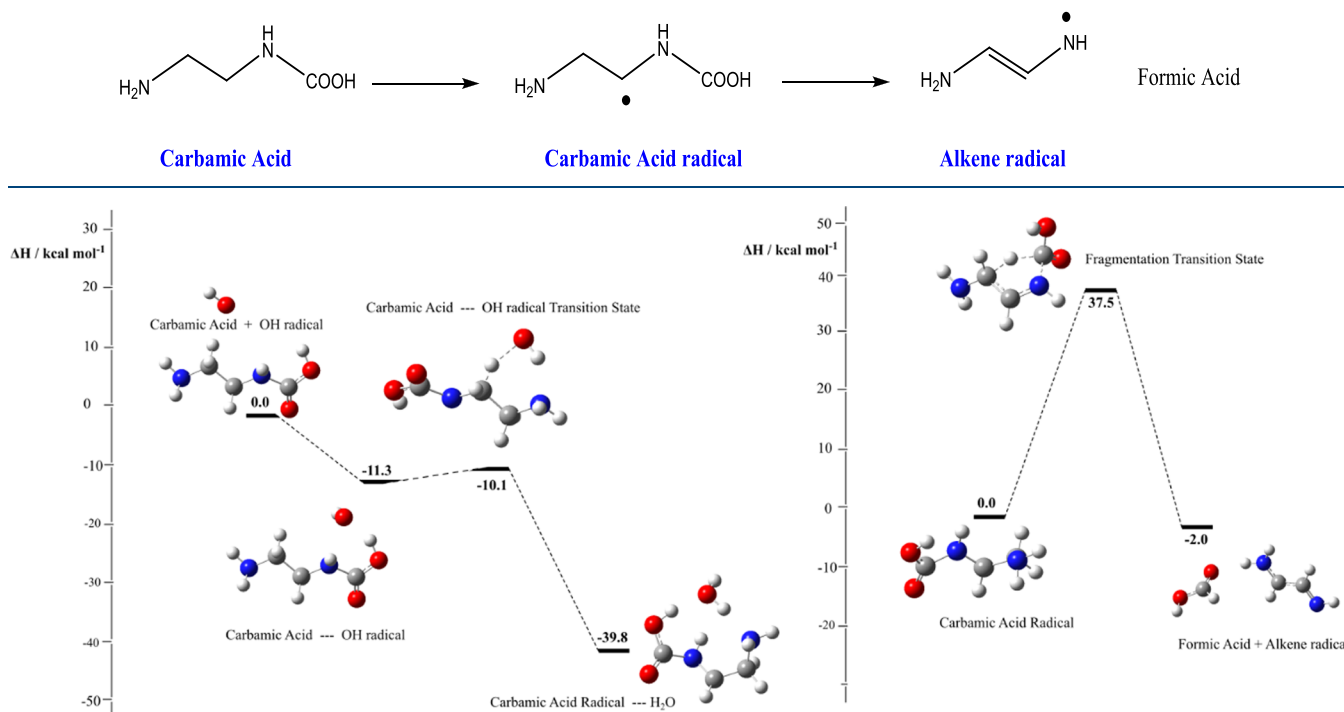
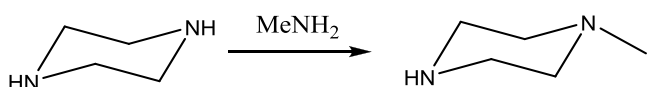


**Figure 19.** DFT-calculated  $\Delta H$  energy profiles for radical abstraction from EDACOOH (left) and fragmentation reaction to release HCOOH (right).

**Scheme 18. Proposed Formation of MPZ from the Reaction of Piperazine and MeNH<sub>2</sub>**



likely occurring in the stripper, can lead to the formation of smaller imines and amines, which in turn are reactants in further substitution reactions.

The modeling studies here will be relevant to the construction of a larger chemical kinetic mechanism. Such a mechanism

would be able to predict both the amount and types of products produced, which in turn could help in selecting a more suitable amine for carbon-capture processes. Key comparisons can be made between the elementary reactions modeled here and current literature data.

Ammonia is a principal reaction product following degradation studies of piperazine. This is consistent with our studies where we have proposed multiple S<sub>N</sub>2 reactions, which involve the formation of ammonia. Furthermore, there are few reactions where ammonia is a reactant, which is consistent with the

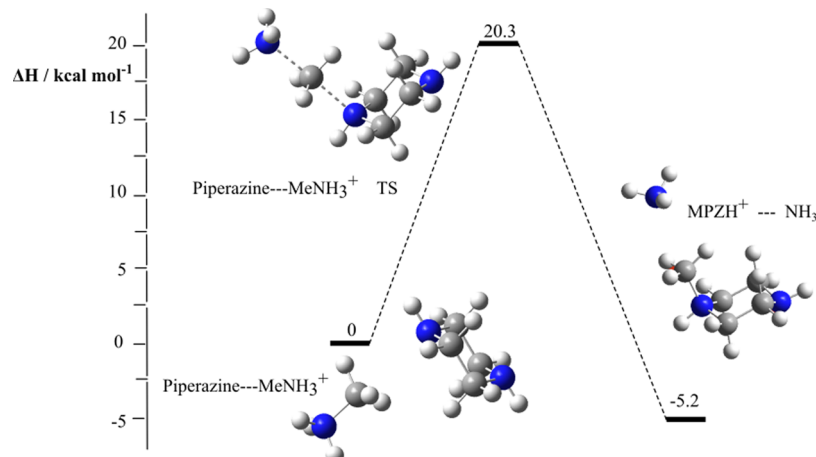


Figure 20. DFT-calculated  $\Delta H$  energy profile for the formation of MPZ.

**Scheme 19. Concerted and Stepwise Routes to the Formation of Nitrosamines**

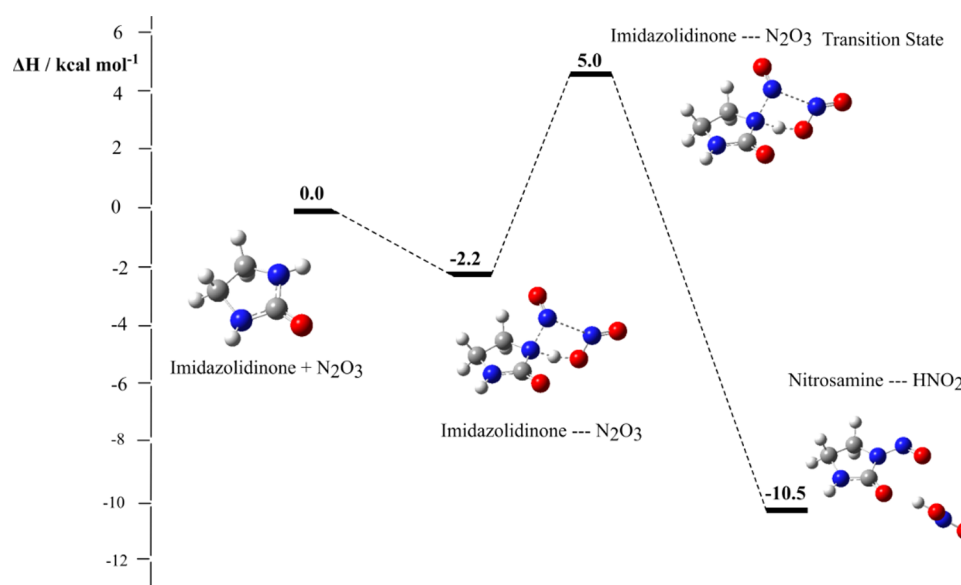
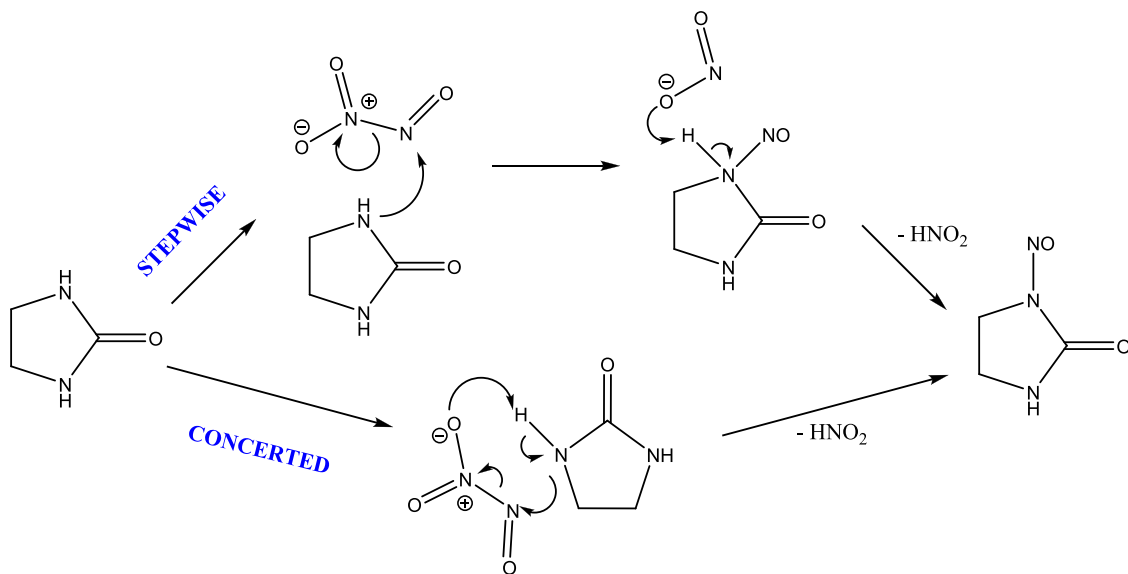


Figure 21. DFT-calculated  $\Delta H$  energy profile for the proposed formation of a nitrosamine from imidazolidinone via a concerted mechanism.

Table 1. Activation Energies for the Formation of Nitrosamines from the Reaction of  $N_2O_3$  with Various Primary and Secondary Amines

Molecule	Reactive site	$\Delta H$ activation energy / kcal mol <sup>-1</sup>
AEI		0.64
		6.62
AEP		8.63
		4.57
Imidazolidinone		7.21
HEP		4.62
AAEFPZ		5.93
		4.57
		8.85

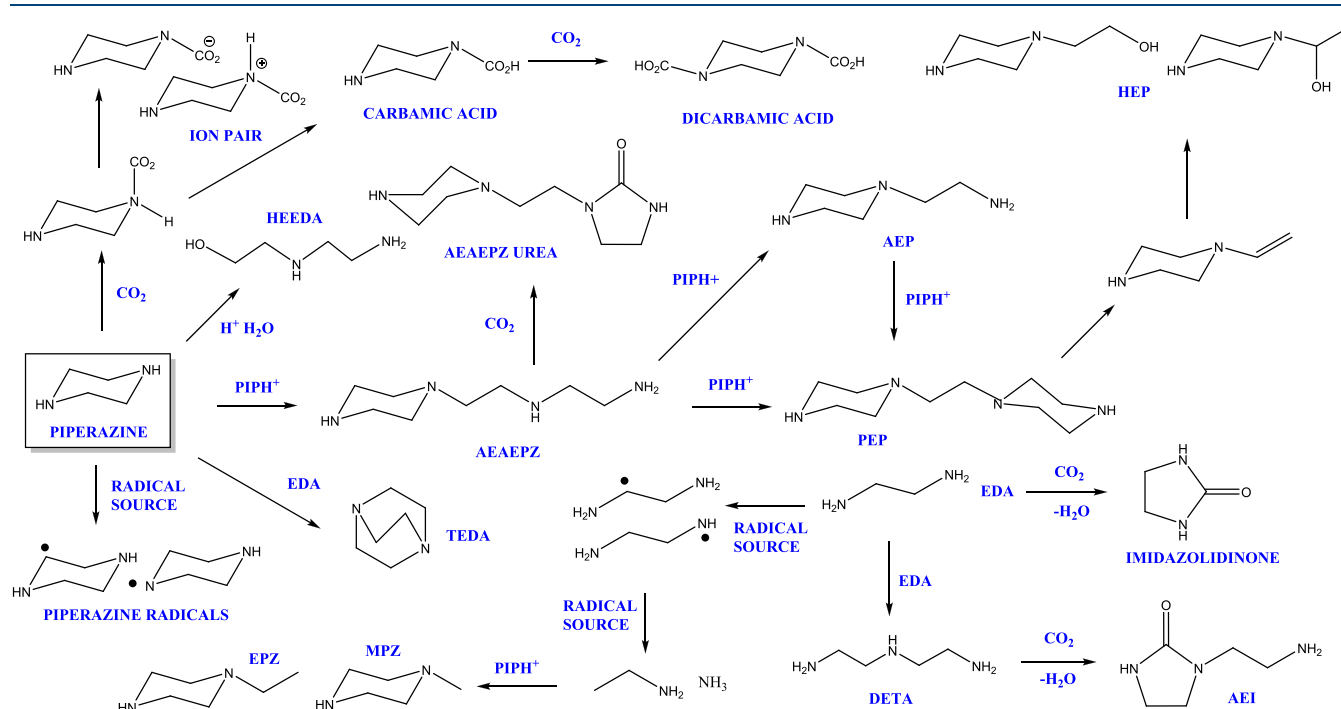


Figure 22. Schematic reaction network detailing the principal interconversions that piperazine and its degradation products can undergo.

experimental observations that ammonia levels increase with time.

HEIA is not observed in experimental studies, which is consistent with our modeling studies that suggest the reaction has a prohibitive activation energy.

Our studies predict that AEP and EDA can form in approximately equal amounts, having similar activation energies.

This, on the face of it, is inconsistent with experimental studies of Freeman et al., where AEP is present in larger concentrations than EDA.<sup>14</sup> However, this is only valid when one considers these steps as singular elementary reactions. It may be accurate that these species are formed in equal amounts initially and that EDA is a reactant in more degradation reactions than AEP is.

The experimental observation that labeled formate and formic acid are formed when  $^{13}\text{CO}_2$  is used as a feedstock cannot completely be explained by our modeling studies. Further work will be needed to deduce further routes to their formation.

## 4. CONCLUSIONS

The current work reports on DFT calculations exploring the formation of multiple thermal and oxidative degradation products of piperazine. Calculated thermodynamic parameters have been compared against experimental conditions to rationalize which pathways are likely and which are unsurmountable.

The chemistry of piperazine degradation is dominated by nucleophilic substitution reactions and can be facilitated by protonation of the amine group. It is shown that some of the reactions are very sensitive to the specific solvent environment of the reactants. Inclusion of explicit water molecules can dramatically reduce the activation parameters.

The mechanistic pathways and corresponding thermodynamic data that have been presented here can form the basis for the construction of a full chemical kinetic model. Such a model would be further improved by corresponding experimental validation studies.

## ■ ASSOCIATED CONTENT

### Supporting Information

The Supporting Information is available free of charge at <https://pubs.acs.org/doi/10.1021/acs.iecr.1c02897>.

Cartesian coordinates for DFT-optimized structures ([PDF](#))

## ■ AUTHOR INFORMATION

### Corresponding Author

**Christopher Parks** – Department of Mechanical Engineering, The University of Sheffield, Sheffield S3 7RD, U.K.;  
[© orcid.org/0000-0001-8016-474X](http://orcid.org/0000-0001-8016-474X); Email: [c.m.parks@sheffield.ac.uk](mailto:c.m.parks@sheffield.ac.uk)

### Authors

**Kevin Hughes** – Department of Mechanical Engineering, The University of Sheffield, Sheffield S3 7RD, U.K.  
**Mohamed Pourkashanian** – Department of Mechanical Engineering, The University of Sheffield, Sheffield S3 7RD, U.K.

Complete contact information is available at:

<https://pubs.acs.org/10.1021/acs.iecr.1c02897>

### Notes

The authors declare no competing financial interest.

## ■ ABBREVIATIONS

AEI	1-(2-aminoethyl)-2-imidazolidone
AEP	N-(2-aminoethyl)piperazine
AAEPZ	1-[2-[(2-aminoethyl)amino] ethyl] piperazine
AAEPZH+	protonated 1-[2-[(2-aminoethyl)amino] ethyl] piperazine
AAEPZ-UREA	1-[2-(piperazinyl)ethyl]-2-imidazolidinone
DETA	1,2-ethanediamine, N1-(2-aminoethyl)
HEIA	N-(2-aminoethyl)-N'-(2-hydroxyethyl)-imidazolidin-2-one)
HEP	N-(2-hydroxyethyl)piperazine

PEP	1,1'-(1,2-ethandiyil)bis-piperazine
PIPH <sup>+</sup>	protonated piperazine
EPZ	N-ethylpiperazine MPZ-N-methylpiperazine
OPZ	2-piperazinone
EDA	ethylenediamine
TEDA	1,4-diazabicyclo[2.2.2]octane

## ■ REFERENCES

- (1) Kerr, R. A. Climate change. Global warming is changing the world. *Science* **2007**, *316*, 188–190.
- (2) Creamer, A. E.; Gao, B. Carbon-Based Adsorbents for Postcombustion CO<sub>2</sub> Capture: A Critical Review. *Environ. Sci. Technol.* **2016**, *50*, 7276–7289.
- (3) Goeppert, A.; Czaun, M.; May, R. B.; Prakash, G. K. S.; Olah, G. A.; Narayanan, S. R. Carbon Dioxide Capture from the Air Using a Polyamine Based Regenerable Solid Adsorbent. *J. Am. Chem. Soc.* **2011**, *133*, 20164–20167.
- (4) Li, K.; White, S.; Zhao, B.; Geng, C.; Halliburton, B.; Wang, Z.; Zhao, Y.; Yu, H.; Yang, W.; Bai, Z.; Azzi, M. Evaluation of a New Chemical Mechanism for 2-Amino-2-methyl-1-propanol in a Reactive Environment from CSIRO Smog Chamber Experiments. *Environ. Sci. Technol.* **2020**, *54*, 9844–9853.
- (5) Hsu, C. S.; Kim, C. J. Diethanolamine (DEA) degradation under gas-treating conditions. *Ind. Eng. Chem. Prod. Res. Dev.* **1985**, *24*, 630–635.
- (6) Kennard, M. L.; Meisen, A. Gas chromatographic technique for analysing partially degraded diethanolamine solutions. *J. Chromatogr. A* **1983**, *267*, 373–380.
- (7) Li, J.; Henni, A.; Tontiwachwuthikul, P. Reaction Kinetics of CO<sub>2</sub> in Aqueous Ethylenediamine, Ethyl Ethanolamine, and Diethyl Monoethanolamine Solutions in the Temperature Range of 298–313 K, Using the Stopped-Flow Technique. *Ind. Eng. Chem. Res.* **2007**, *46*, 4426–4434.
- (8) Wang, Z.; Fang, M.; Pan, Y.; Yan, S.; Luo, Z. Amine-based absorbents selection for CO<sub>2</sub> membrane vacuum regeneration technology by combined absorption–desorption analysis. *Chem. Eng. Sci.* **2013**, *93*, 238–249.
- (9) Zhou, S.; Chen, X.; Nguyen, T.; Voice, A. K.; Rochelle, G. T. Aqueous Ethylenediamine for CO<sub>2</sub> Capture. *ChemSusChem* **2010**, *3*, 913–918.
- (10) Chakma, A.; Meisen, A. Identification of methyl diethanolamine degradation products by gas chromatography and gas chromatography–mass spectrometry. *J. Chromatogr. A* **1988**, *457*, 287–297.
- (11) Ogidi, M. O.; Thompson, W. A.; Maroto-Valer, M. M. Thermal Degradation of Morpholine in CO<sub>2</sub> Post-combustion Capture. *Energy Procedia* **2017**, *114*, 1033–1037.
- (12) Liu, K.; Jinka, K. M.; Remias, J. E.; Liu, K. Absorption of Carbon Dioxide in Aqueous Morpholine Solutions. *Ind. Eng. Chem. Res.* **2013**, *52*, 15932–15938.
- (13) Mazari, S. A.; Abro, R.; Bhutto, A. W.; Saeed, I. M.; Ali, B. S.; Jan, B. M.; Ghalib, L.; Ahmed, M.; Mubarak, N. M. Thermal degradation kinetics of morpholine for carbon dioxide capture. *J. Environ. Chem. Eng.* **2020**, *8*, No. 103814.
- (14) Freeman, S. A.; Dugas, R.; Van Wagener, D. H.; Nguyen, T.; Rochelle, G. T. Carbon dioxide capture with concentrated, aqueous piperazine. *Int. J. Greenhouse Gas Control* **2010**, *4*, 119–124.
- (15) Nguyen, T.; Hilliard, M.; Rochelle, G. T. Amine volatility in CO<sub>2</sub> capture. *Int. J. Greenhouse Gas Control* **2010**, *4*, 707–715.
- (16) Rochelle, G.; Chen, E.; Freeman, S.; Van Wagener, D.; Xu, Q.; Voice, A. Aqueous piperazine as the new standard for CO<sub>2</sub> capture technology. *Chem. Eng. J.* **2011**, *171*, 725–733.
- (17) Freeman, S. A.; Davis, J.; Rochelle, G. T. Degradation of aqueous piperazine in carbon dioxide capture. *Int. J. Greenhouse Gas Control* **2010**, *4*, 756–761.
- (18) Wilk, A.; Więćław-Solny, L.; Tatarczuk, A.; Krótki, A.; Spietz, T.; Chwola, T. Solvent selection for CO<sub>2</sub> capture from gases with high carbon dioxide concentration. *Korean J. Chem. Eng.* **2017**, *34*, 2275–2283.

- (19) Rao, A. B.; Rubin, E. S. A Technical Economic, and Environmental Assessment of Amine-Based CO<sub>2</sub> Capture Technology for Power Plant Greenhouse Gas Control. *Environ. Sci. Technol.* **2002**, *36*, 4467–4475.
- (20) Freeman, S. A.; Rochelle, G. T. Thermal Degradation of Aqueous Piperazine for CO<sub>2</sub> Capture: 2. Product Types and Generation Rates. *Ind. Eng. Chem. Res.* **2012**, *51*, 7726–7735.
- (21) Matsuzaki, Y.; Yamada, H.; Chowdhury, F. A.; Higashii, T.; Onoda, M. Ab Initio Study of CO<sub>2</sub> Capture Mechanisms in Aqueous Monoethanolamine: Reaction Pathways for the Direct Interconversion of Carbamate and Bicarbonate. *J. Phys. Chem. A* **2013**, *117*, 9274–9281.
- (22) Yamada, H.; Matsuzaki, Y.; Higashii, T.; Kazama, S. Density Functional Theory Study on Carbon Dioxide Absorption into Aqueous Solutions of 2-Amino-2-methyl-1-propanol Using a Continuum Solvation Model. *J. Phys. Chem. A* **2011**, *115*, 3079–3086.
- (23) Yang, X.; Rees, R. J.; Conway, W.; Puxty, G.; Yang, Q.; Winkler, D. A. Computational Modeling and Simulation of CO<sub>2</sub> Capture by Aqueous Amines. *Chem. Rev.* **2017**, *117*, 9524–9593.
- (24) Yoon, B.; Stowe, H. M.; Hwang, G. S. Molecular mechanisms for thermal degradation of CO<sub>2</sub>-loaded aqueous monoethanolamine solution: a first-principles study. *Phys. Chem. Chem. Phys.* **2019**, *21*, 22132–22139.
- (25) Vevelstad, S. J.; Eide-Haugmo, I.; da Silva, E. F.; Svendsen, H. F. Degradation of MEA; a theoretical study. *Energy Procedia* **2011**, *4*, 1608–1615.
- (26) Saeed, I. M.; Lee, V. S.; Mazari, S. A.; Si Ali, B.; Basirun, W. J.; Asghar, A.; Ghalib, L.; Jan, B. M. Thermal degradation of aqueous 2-aminoethylethanamine in CO<sub>2</sub> capture; identification of degradation products, reaction mechanisms and computational studies. *Chem. Cent. J.* **2017**, *11*, No. 10.
- (27) Yoon, B.; Hwang, G. S. On the mechanism of predominant urea formation from thermal degradation of CO<sub>2</sub>-loaded aqueous ethylenediamine. *Phys. Chem. Chem. Phys.* **2020**, *22*, 17336–17343.
- (28) Parks, C.; Alborzi, E.; Akram, M.; Pourkashanian, M. DFT Studies on Thermal and Oxidative Degradation of Monoethanolamine. *Ind. Eng. Chem. Res.* **2020**, *59*, 15214–15225.
- (29) Frisch, M. J.; Trucks, G. W.; Schlegel, H. B.; Scuseria, G. E.; Robb, M. A.; Cheeseman, J. R.; Scalmani, G.; Barone, V.; Mennucci, B.; Petersson, G. A.; Nakatsuji, H.; Caricato, M.; Li, X.; Hratchian, H. P.; Izmaylov, A. F.; Bloino, J.; Zheng, G.; Sonnenberg, J. L.; Hada, M.; Ehara, M.; Toyota, K.; Fukuda, R.; Hasegawa, J.; Ishida, M.; Nakajima, T.; Honda, Y.; Kitao, O.; Nakai, H.; Vreven, T.; Montgomery, J. J. A.; Peralta, J. E.; Ogliaro, F.; Bearpark, M.; Heyd, J. J.; Brothers, E.; Kudin, K. N.; Staroverov, V. N.; Keith, T.; Kobayashi, R.; Normand, J.; Raghavachari, K.; Rendell, A.; Burant, J. C.; Iyengar, S. S.; Tomasi, J.; Cossi, M.; Rega, N.; Millam, J. M.; Klene, M.; Knox, J. E.; Cross, J. B.; Bakken, V.; Adamo, C.; Jaramillo, J.; Gomperts, R.; Stratmann, R. E.; Yazyev, O.; Austin, A. J.; Cammi, R.; Pomelli, C.; Ochterski, J. W.; Martin, R. L.; Morokuma, K.; Zakrzewski, V. G.; Voth, G. A.; Salvador, P.; Dannenberg, J. J.; Dapprich, S.; Daniels, A. D.; Farkas, O.; Foresman, J. B.; Ortiz, J. V.; Cioslowski, J.; Fox, D. J. *Gaussian 09*, revision D.01; Gaussian, Inc.: Wallingford, CT, 2016.
- (30) Lee, C.; Yang, W.; Parr, R. G. Development of the Colle-Salvetti correlation-energy formula into a functional of the electron density. *Phys. Rev. B: Condens. Matter Mater. Phys.* **1988**, *37*, 785–789.
- (31) Dunning, T. H., Jr. Gaussian basis sets for use in correlated molecular calculations. I. The atoms boron through neon and hydrogen. *J. Chem. Phys.* **1989**, *90*, 1007–1023.
- (32) Galano, A.; Alvarez-Idaboy, J. R. Kinetics of radical-molecule reactions in aqueous solution: A benchmark study of the performance of density functional methods. *J. Comput. Chem.* **2014**, *35*, 2019–2026.
- (33) Mangiatordi, G. F.; Brémond, E.; Adamo, C. DFT and Proton Transfer Reactions: A Benchmark Study on Structure and Kinetics. *J. Chem. Theory Comput.* **2012**, *8*, 3082–3088.
- (34) Zhao, Y.; Truhlar, D. G. The M06 suite of density functionals for main group thermochemistry, thermochemical kinetics, noncovalent interactions, excited states, and transition elements: two new functionals and systematic testing of four M06-class functionals and 12 other functionals. *Theor. Chem. Acc.* **2008**, *120*, 215–241.
- (35) Scalmani, G.; Frisch, M. J. Continuous surface charge polarizable continuum models of solvation. I. General formalism. *J. Chem. Phys.* **2010**, *132*, No. 114110.
- (36) Grimme, S.; Ehrlich, S.; Goerigk, L. Effect of the damping function in dispersion corrected density functional theory. *J. Comput. Chem.* **2011**, *32*, 1456–1465.
- (37) Cancès, E.; Mennucci, B.; Tomasi, J. A new integral equation formalism for the polarizable continuum model: Theoretical background and applications to isotropic and anisotropic dielectrics. *J. Chem. Phys.* **1997**, *107*, 3032–3041.
- (38) Funes-Ardoiz, I.; Paton, R. S. Good Vibes: Version 2.0.3. Zenodo, 2018.
- (39) Bedell, S. A.; Worley, C. M.; Al-Horr, R. S.; McCrary, D. A. Quaternaries as Intermediates in the Thermal and Oxidative Degradation of Alkanolamines. *Ind. Eng. Chem. Res.* **2010**, *49*, 7147–7151.
- (40) Gouedard, C.; Picq, D.; Launay, F.; Carrette, P. L. Amine degradation in CO<sub>2</sub> capture. I. A review. *Int. J. Greenhouse Gas Control* **2012**, *10*, 244–270.
- (41) Lepaumier, H.; Picq, D.; Carrette, P.-L. New Amines for CO<sub>2</sub> Capture. II. Oxidative Degradation Mechanisms. *Ind. Eng. Chem. Res.* **2009**, *48*, 9068–9075.
- (42) Wright, J. S.; Ingold, K. U. Understanding Trends in C-H, N-H, and O-H Bond Dissociation Enthalpies. *J. Chem. Educ.* **2000**, *77*, No. 1062.
- (43) Dai, N.; Mitch, W. A. Influence of amine structural characteristics on N-nitrosamine formation potential relevant to postcombustion CO<sub>2</sub> capture systems. *Environ. Sci. Technol.* **2013**, *47*, 13175–13183.
- (44) Dai, N.; Shah, A. D.; Hu, L.; Plewa, M. J.; McKague, B.; Mitch, W. A. Measurement of Nitrosamine and Nitramine Formation from NO<sub>x</sub> Reactions with Amines during Amine-Based Carbon Dioxide Capture for Postcombustion Carbon Sequestration. *Environ. Sci. Technol.* **2012**, *46*, 9793–9801.
- (45) Fine, N. A.; Goldman, M. J.; Rochelle, G. T. Nitrosamine formation in amine scrubbing at desorber temperatures. *Environ. Sci. Technol.* **2014**, *48*, 8777–8783.
- (46) Fine, N. A.; Nielsen, P. T.; Rochelle, G. T. Decomposition of nitrosamines in CO<sub>2</sub> capture by aqueous piperazine or monoethanolamine. *Environ. Sci. Technol.* **2014**, *48*, 5996–6002.
- (47) Goldman, M. J.; Fine, N. A.; Rochelle, G. T. Kinetics of N-Nitrosopiperazine Formation from Nitrite and Piperazine in CO<sub>2</sub> Capture. *Environ. Sci. Technol.* **2013**, *47*, 3528–3534.
- (48) Shi, H.; Supap, T.; Idem, R.; Gelowitz, D.; Campbell, C.; Ball, M. Nitrosamine Formation in Amine-Based CO<sub>2</sub> Capture in the Absence of NO<sub>2</sub>: Molecular Modeling and Experimental Validation. *Environ. Sci. Technol.* **2017**, *51*, 7723–7731.